KARMA

Karst **A**quifer **R**esources availability and quality in the **M**editerranean **A**rea

Validation of individual EWS for spring and system efficiency assessment

Deliverable 3.3

Authors:

Juan Antonio Barberá Fornell (UMA), Christelle Batiot-Guilhe (UMO) Michele Citton (AUB), Joanna Doummar (AUB), Simon Frank (KIT), Nadine Goeppert (KIT), Nikolai Fahrmeier (KIT) & Nico Goldscheider (KIT), Hervé Jourde (UMO), Bartolomé Andreo Navarro (UMA), Jaime Fernández Ortega (UMA), Jihad Othman (AUB), Jean-Luc Seidel (UMO), Xiaoguang Wang (UMO), Naomi Mazzilli (UMO)

Date: April 2022

This project has received funding from the European Union's PRIMA research and innovation programme

Technical References

Project Acronym	**KARMA**
EU Programme, Call and Topic	PRIMA, Multi-topic 2018, Water resources availability and quality within catchments and aquifers
Project Title	Karst Aquifer Resources availability and quality in the Mediterranean Area
Project Coordinator	Prof. Dr. Nico Goldscheider, Karlsruhe Institute of Technology (KIT), nico.goldscheider@kit.edu
Project Duration	September 2019 - August 2022
Deliverable No., Name	D3.3 Validation of individual EWS for spring and system efficiency assessment
Dissemination Level	PU (public)
Work Package	WP3: Water Quality
Task	Task 3.2 Early-warning systems (EWS) for spring water contamination
Lead beneficiary	University of Malaga (UMA)
Contributing beneficiary/ies	Karlsruhe Institute of Technology (KIT), University of Montpellier (UM) and Sapienza University of Rome (URO)
Due Date	Month 30
Actual Submission Date	Month 32

Version History

Version	Date
1.0	May 2022

Project Partners

(Coordinator)

Executive Summary

This third deliverable of WP3 (Water Quality) deals with the validation of individual Early Warning System (EWS) and system efficiency assessment in selected water supplies across the Mediterranean area. At individual test sites, Gran Sasso aquifer (Italy), Ubrique test site (Spain), Lez spring (France) and Hochifen-Gottesacker karst area (Austria), different datasets of hydrogeologicalparameters have been recorded and analyzed to identify those with the highest correlation with contamination in each site.

Despite that the four KARMA study cases for EWS development present different characteristics, the methodological procedure applied in all of them is quite similar. In Deliverable 3.1, the main description of the monitoring network at each study area is included, and then, in Deliverable 3.2, the characteristics of the karst groundwater supply, description of water quality issues and available background knowledge are described. It is observed that, beside the specificity of each site, turbidity is the common physical property of groundwater that hinders its usage for human consumption. Maximum turbidity values of ≈140 NTU were recorded at Vitella D'Oro spring (Italy), ≈60 NTU at Cornicabra spring, ≈300 NTU at Algarrobal spring (Ubrique test site, Spain), ≈150 NTU at Lez spring (France) and ≈25 at Sägebach spring (Austria). The consumption of groundwater from Vitella D'Oro springs requires the use of physical filters to avoid drinking water quality impairment during intense turbidity events. In the case of Ubrique test site, the detection of high bacterial activity together with turbidity totally impede groundwater exploitation during short periods. At Lez spring, different groundwater origins are identified (superficial circulation within the main aquifer, water coming from deep circulation, surface-water interactions and surface waters polluted by anthropogenic effluents), so that turbidity monitoring is not enough to discriminate the arrival of contaminants. In the Austrian test site, an apparently good correlation between particle size distribution and turbidity together with β-d-glucuronidase is shown, which can be thus considered highly suitable parameters for an early-warning system regarding bacterial contamination.

Table of contents

1 Introduction

The overarching objective of the KARMA project is to achieve substantial progress in the hydrogeological understanding and sustainable management of karst groundwater resources in the Mediterranean area in terms of water availability and quality. At karst catchment scale, the main objective is to advance and compare transferable modeling tools for improved predictions of climate-change impacts and better-informed water management decisions, and to prepare vulnerability maps as tools for groundwater quality protection.

In order to accomplish the objectives established in WP3, novel research focused on water quality will be tested at four selected Mediterranean karst aquifers of distinctive geographical, geological and climatological contexts (Fig 1.1). These test sites selected for KARMA project show similar features regarding groundwater use (drinking water supply, crop irrigation) and face the same threats (pollution episodes, climate change). Thus, Early Warning Systems (EWS) have emerged as a promising tool to detect groundwater low quality periods or contamination events in drinking water sources, but they have been little tested in groundwater supply systems. In particular, karst aquifers show certain similarities with surface water systems (hierarchized drainage, fast flow dynamic, high vulnerability to contamination, etc.) that make them ideal for EWS development.

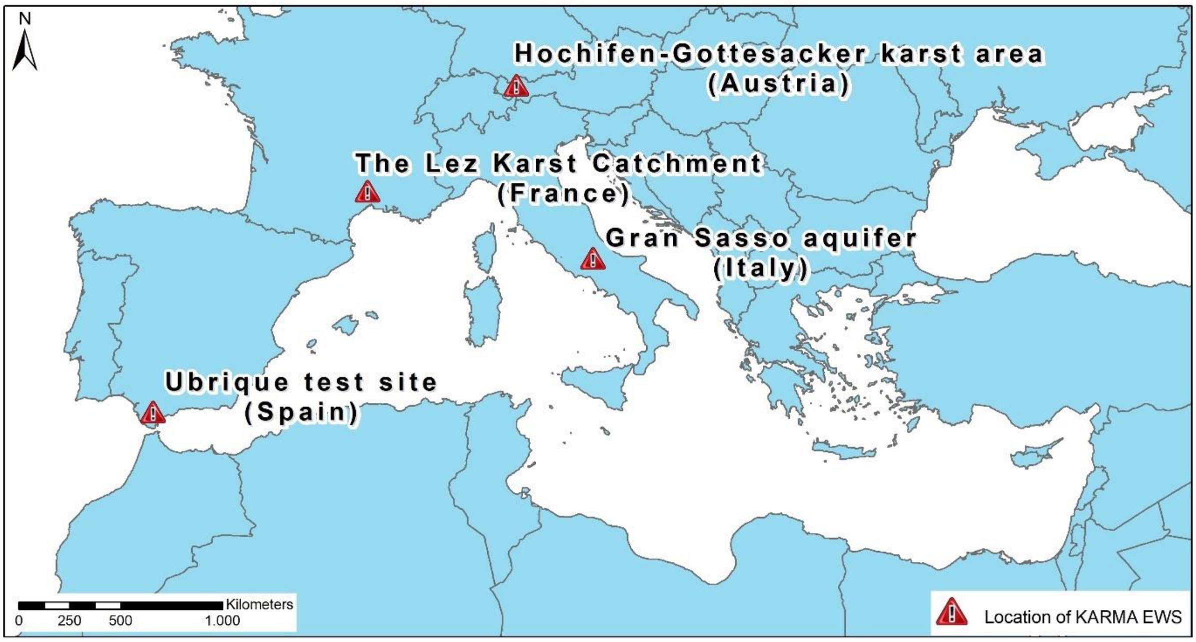

Figure 1.1. Location map of selected test sites in Karma project for Early Warning System development and implementation.

The four KARMA Early Warning System test sites share the application of some methods used to detect contamination events, specifically the use of fluorescence-based techniques. The field device mostly used, a field fluorometer (GGUN from Albillia Sarl., Switzerland), consist on a submersible probe connected to a digital data logger. In most cases, the device's sampling rate is approximately 15 minutes. The use of this kind of field equipment allows to configure the optical channels which better work for each test site (protein-like fluorescence, uranine, rhodamine, DOM, turbidity…). These specific features together with the inexpensive and fast measurements of the field fluorometer, make this approach ideal for water quality monitoring tasks.

2 The Gran Sasso aquifer (Case Study Italy)

2.1 Hydrogeological setting

The Gran Sasso carbonate aquifer is defined as the most representative karst aquifer of the central Apennines, for its huge amount of water resources and the interaction between groundwater and underground works (Celico, 2005). The Gran Sasso aquifer is characterised by high permeability due to fracturing and karstification and by the high effective infiltration that feeds important springs located at its boundary (Amoruso, 2012). The groundwater resources are mainly exploited for human purposes and partially drained by highway tunnels (Celico et al., 2005; Figure 2.1).

The Gran Sasso springs were classified into six groups (Gr in Figure 2.1) according to their hydrogeological setting and hydrochemistry (Barbieri et al., 2005, Tallini et al., 2013) (Figure 2.1). The total discharge from its springs is between 18 m3/s and 25 m3/s and corresponds to a net infiltration of about 800 mm/year (Amoruso et al., 2012). The Gran Sasso aquifer is characterised by a hydraulic conductivity of 10−6–10−7 m/s and a regional hydraulic gradient of 5–20 ‰ (Amoruso et al., 2012). At the massif core, an endorheic basin having a tectonic-karst origin, called Campo Imperatore basin (elevation 1650 m a.s.l), acts as preferential recharge area of the Gran Sasso aquifer, fed by high rainfall and snow rate.

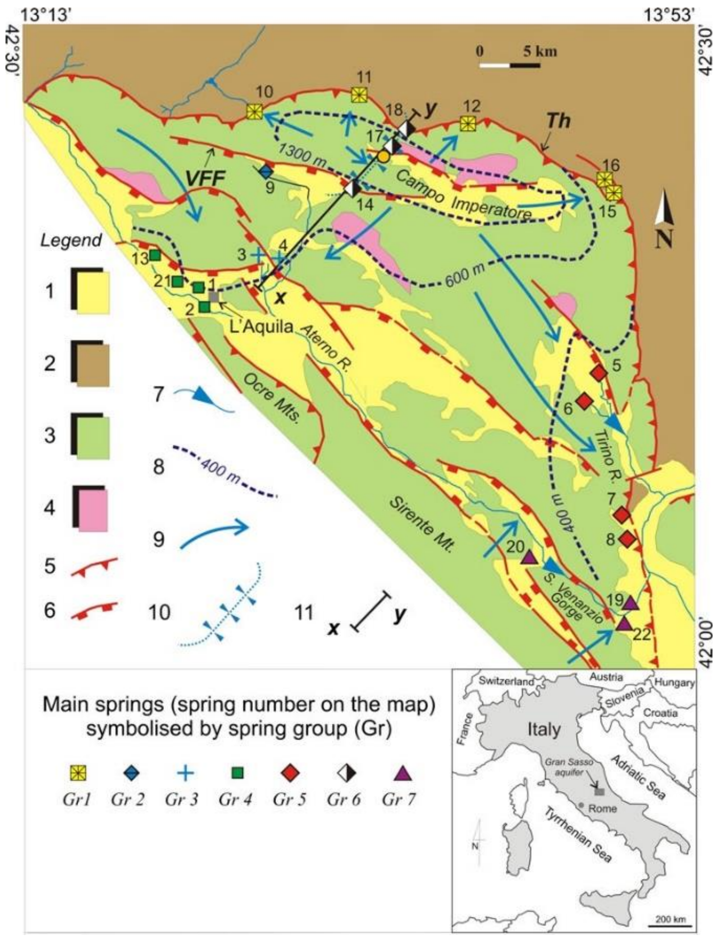

Figure 2.1: GSCA hydrogeological framework. 1) Aquitard (continental detrital units of intramontane basins, Quaternary), 2) aquiclude (terrigenous turbidites, Mio- Pliocene), 3) aquifer (calcareous sequences, Meso-Cenozoic), 4) low permeability bedrock (dolomite, upper Triassic), 5) thrust, 6) extensional fault, 7) streambed spring, 8) presumed water table elevation (in m a.s.l.), 9) regional groundwater flowpath, 10) highway tunnels drainage. Gr1-Gr7 are the main springs (Tallini et al., 2013)

2.2 EWS study case: Vitella D'Oro spring

Springs of the Tavo River basin (Vitella D'Oro and Mortaio D'Angri springs, number 15 and 16 in Figure 2.1) are located at an altitude of about 700 m a.s.l. (Figure 2.2). The analysis of the bibliographic data of the flow rates and the comparison with the rainfall have highlighted the karst behaviour of the springs group (Ferracuti et al., 2006). In fact, monitoring of flow rates and chemical-physical parameters of the Tavo river waters identifies significant water exchanges between the limestone complex, representing the regional aquifer, and the Rigopiano conglomerates, which only partially drains the aquifer (Figure 2.2). The water circulating in the conglomerates, is carried through karstic circuits towards to the Vitella d'Oro spring (Ferracuti et al., 2006). During the study of the karst circuits spring, it was observed that Vitella d'Oro spring is characterized by water turbidity (Rusi et al., 2016).

The hydrogeology and hydrodynamics of the surface karst flow are responsible for the turbidity in the Tavo spring. This phenomenon triggers the use of filters to preserve the drinking water quality during the most intense turbidity events. This condition occurs mainly in the Vitella d'Oro basin occasionally and after intense and long-lasting rainfall events that cause increases in flow rate, especially in the fall period.

Ferracuti et al. (2006) assumed that the average delay between the time of flow increase and the time when turbidity is triggered is approximately three hours and a half. The delay ranges between a minimum of less than one hour and a maximum of nine hours.

The possibility of a second turbidity peak occurrence was also observed, which generally is recorded between six and eleven hours after the first arrival of turbidity. Only in particularly dry years, when rainfall is poorly distributed (e.g. heavy rainfall after long dry periods), there is a perfect match between rainfall and turbidity.

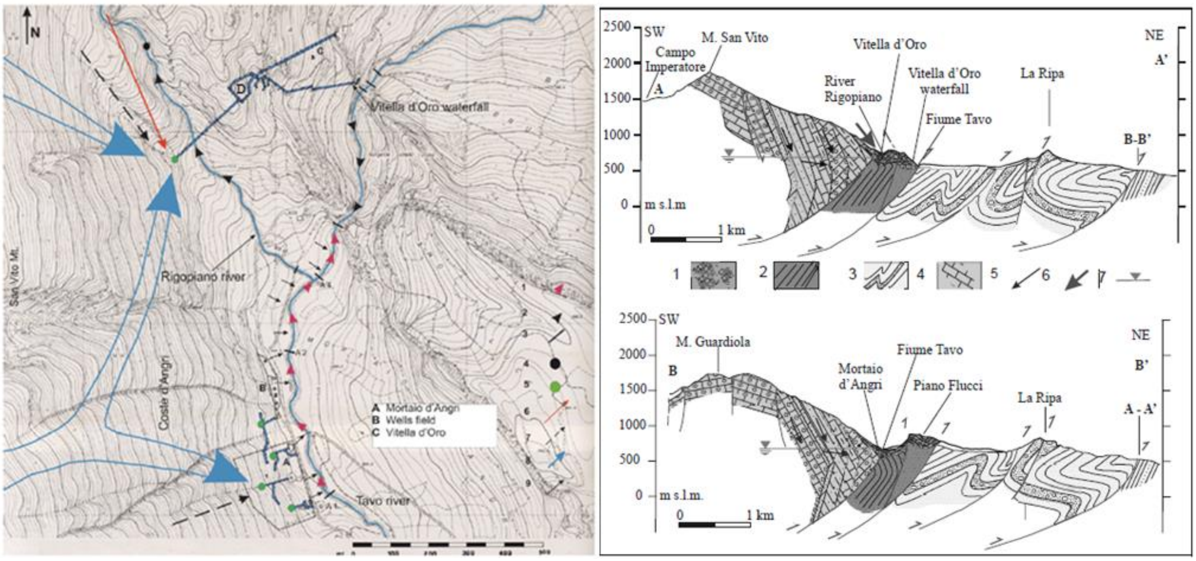

Figure 2.2: On the left side: hydrodynamic scheme. A) Mortaio d'Angri, B) Wells field, C) Vitella d'Oro, D) Vitella D'oro spring catchment tank 1) Linear springs, 2) decrease of discharge, 3) sections of discharge measurement, 4) swallow hole, 5) catchments, 6) karstic circuit responsible of turbidity from Rigopiano river, 7) karstic circuit, 8) directions of the basal flow, 9) groundwater interactions between the carbonate and Rigopiano conglomerate complexes (Rusi et al., 2016). On the right side: Geologic - hydrogeologic cross-sections. 1) Conglomerate of Rigopiano complex, 2) Calcareniti di M.Fiore complex, 3) Laga and Cellino complex, 4) calcareous complex, 5) karstic conduits responsible of the floods, 6) karstic conduits responsible of turbidity, 7) Springs altitude (661,4 m Vitella d'Oro - 675 m Mortaio d'Angri)(Ferracuti, 2016).

In order to monitor turbidity and the correlation between turbidity and precipitation/outflow rate, an Albillia FL30 Fluorometer probe was installed in the Vitella d'Oro spring (Figure 2.3). The probe is a continuous flow field fluorometer that allows continuous monitoring of several tracers (up to a maximum of three). In addition to these, a turbidity-independent measurement is implemented (Schnegg, 2002). The main advantage of this field instrument is the immediate availability of the data (flash memory) (Schnegg, 2002). The probe is connected to a data recorder and the signal is digitally transferred to a laptop only via an infrared interface. The acquisition time of the field fluorometer was set every 15 minutes.

Figure 2.3: Location of Fluorometer probe (Vitella d'Oro spring catchment)

In Figure 2.4 time series of discharge, rainfall (on a daily basis), turbidity, temperature and electrical conductivity (every 15 minutes) were displayed. The acquiring data period was from 28th April 2021 to 4th February 2022. From April 2021 until October 2021 the discharge rate, turbidity, temperature and electrical conductivity values are defined by steady-state conditions (temperature ≈ 7.5 °C, electrical conductivity ≈ 300 µS/cm and turbidity ≤ 1 NTU). In particular, the discharge rate was below 0.4 m3/s and it is characterized by a slight decrease trend from 0.4 m3/s to 0.2 m3/s. Starting since October 2021 the increase in rainfall induced discharge increase and consequently also in turbidity and electrical conductivity values. During the monitoring period, two main step changes are clearly detectable. The first one starts on 8th October 2021, while the second one starts on 16th November 2021. It is noteworthy that the rainfall event recorded on 17th July 2021, despite the intensity of 64 mm/day, did not induced any changes in the spring parameters. According to Rusi et al., 2016 a single rainy day is not enough to trigger turbidity events at the Vitella D'Oro spring.

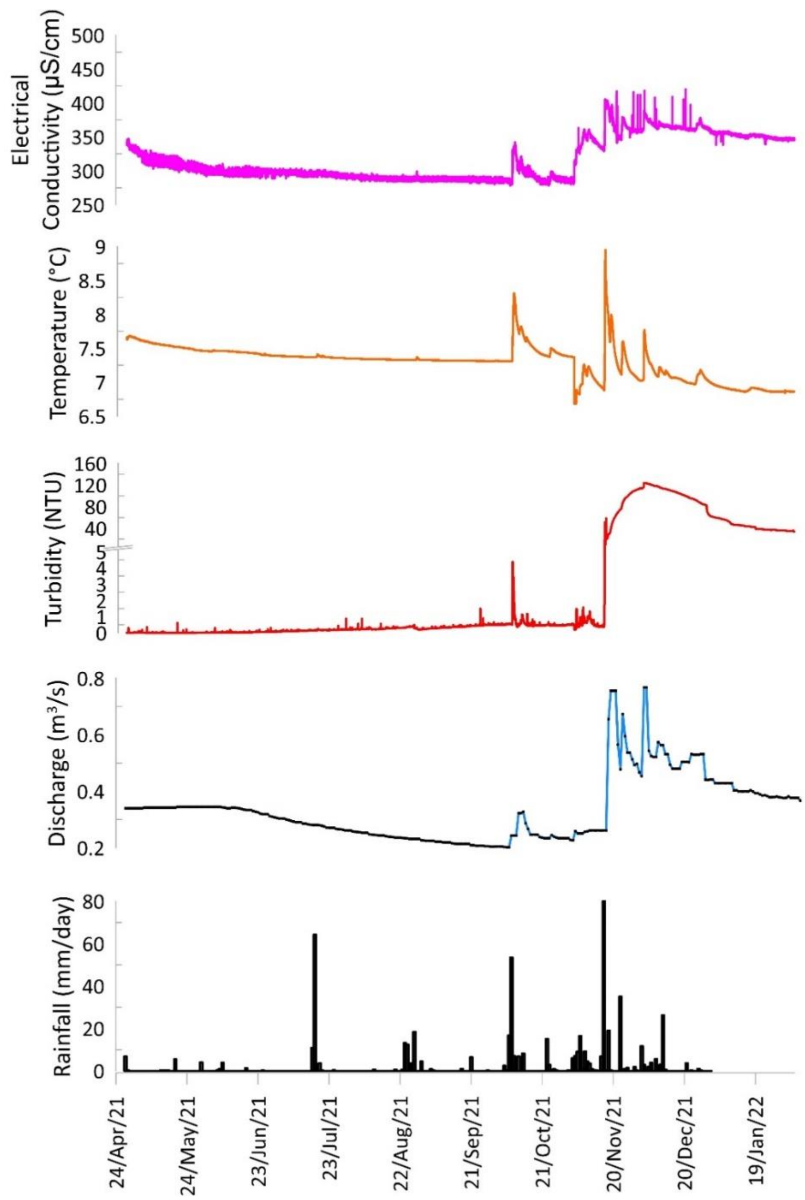

Figure 2.4: Vitella D'Oro Time series. Note that the turbidity scale (y-axis) is subdivided into two ranges, from 0 NTU to 5 NTU and from 40 NTU to 160 NTU, in order to improve the amplification and observation of the small variations.

In Figure 2.5 the 8th October 2021 the event affecting discharge, turbidity, temperature and electrical conductivity, induced by rainfall event of 53 mm/day is displayed. The maximum change in turbidity recorded is 4.37 NTU. The turbidity variation period lasts a day, since 8th October 2021 h 9:00 to 9th October 2021 h 9:30. The lag time between rainfall and parameters changes is not exactly detected because the rainfall sample data set has a daily basis. The increases in temperature and electrical conductivity are due to the arrival of rainfall water that has crossed the Conglomerates of Rigopiano formation before reaching the aquifer.

In Figure 2.6, the 16th November 2021 step changes of discharge, turbidity, temperature and electrical conductivity induced by rainfall event of 80 mm/day are displayed. Since 16th November 2021 to January 2022 the discharge and the turbidity are characterized by values higher than data recorded before the rainfall event. It is noteworthy that despite temperature and discharge come back to low values, turbidity remains on higher values. This is possibly due to mud on the sensor.

The study of this sector of the Gran Sasso aquifer allows to better describe how a karstic system like Vitella D'Oro one is influenced by rapid flowpath from recharge to discharge areas. The cross-correlation performed on chemical-physical parameters shows that at least one day occurs between the rainfall and turbidity events. This finding also confirms the above-mentioned contributions (Ferracuti et al., 2006; Rusi et al., 2016). This means that a karst system like Vitella d'Oro is extremely vulnerable with respect to potential contamination events in the recharge area. Eventually, a potential contaminant can quickly reach the spring and the water resource cannot be useful for human purposes.

In addition to this, a tracer test is planned on March 2022 to check the travel time of the water from the recharge basin to the spring. The results of these tests will help to determine the EWS system at Vitella d'Oro spring.

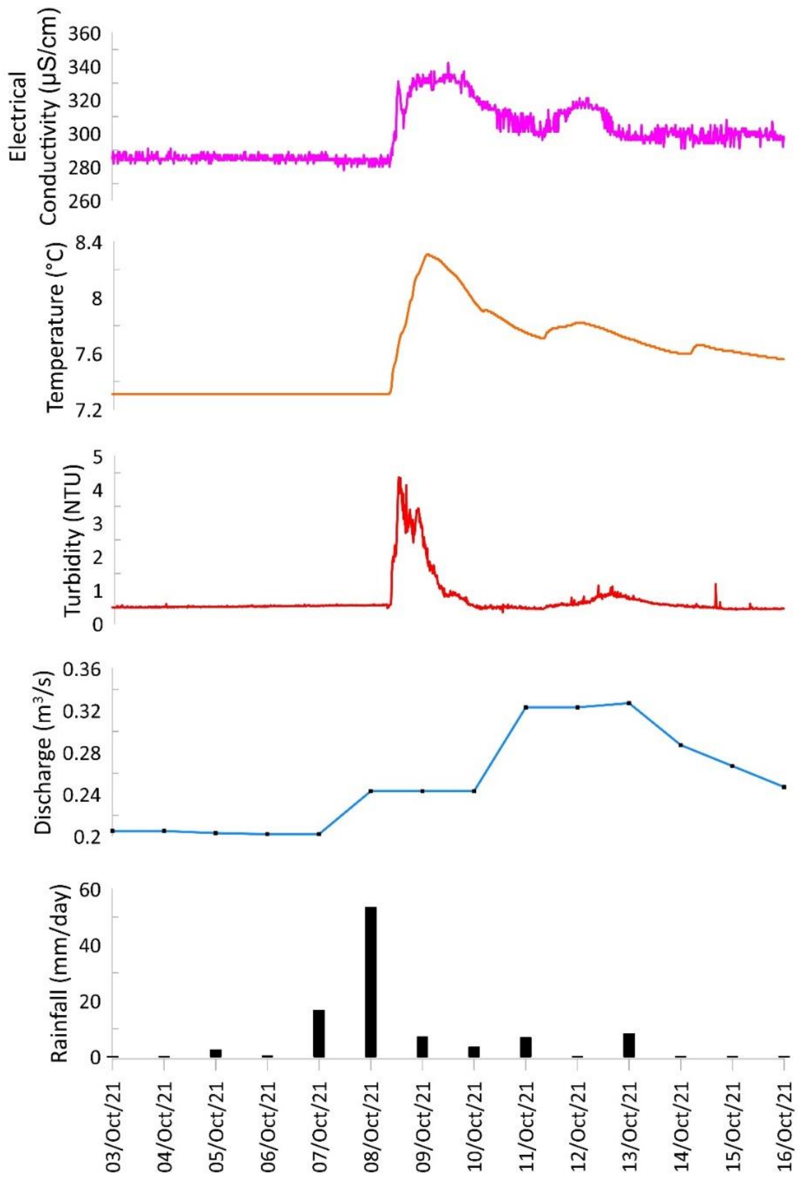

Figure 2.5: Changes in Vitella D'Oro Time series in October 2021

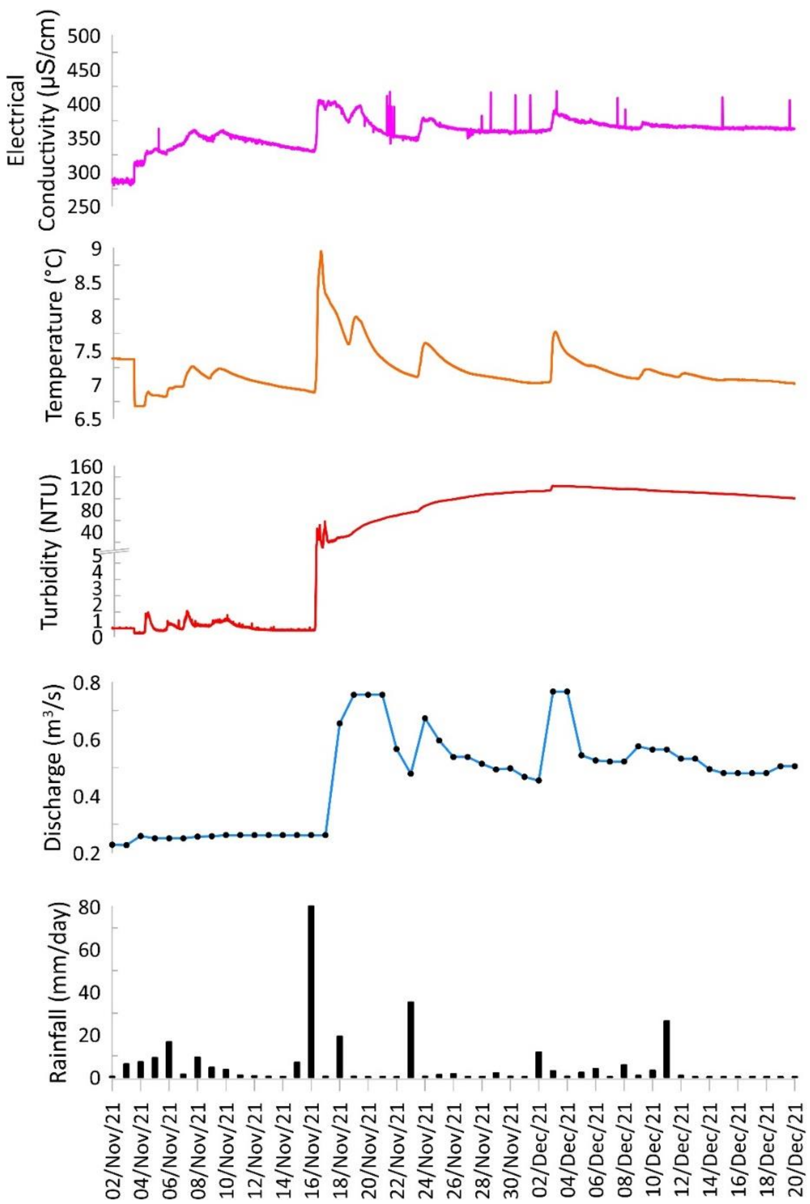

Figure 2.6: Changes in Vitella D'Oro Time series in November/December 2021

2.3 References

Amoruso, A., Crescentini, L., Petitta, M., & Tallini, M. (2012). Parsimonious recharge/discharge modeling in carbonate fractured aquifers: The groundwater flow in the Gran Sasso aquifer (Central Italy). Journal of Hydrology, 476, 136–146.

Adinolfi Falcone R., Falgiania A., Marco Petitta M. and Marco Tallini (2006). Characteristics of the Gran Sasso INFN laboratory groundwater (inferred from 1996-1998 spot sampling data) to fine-tune the conceptual model of water-rock interaction in carbonate aquifers.

Barbieri, M., Boschetti, T., Petitta, M., & Tallini, M. (2005). Stable isotope (2H, 18O and 87Sr/ 86Sr) and hydrochemistry monitoring for groundwater hydrodynamics analysis in a karst aquifer (Gran Sasso, Central Italy). Applied Geochemistry, 20(11), 2063–2081.

Celico, P., Fabbrocino, S., Petitta, M., & Tallini, M. (2005). Hydrogeological impact of the Gran Sasso motor-way tunnels (Central Italy). Giornale Di Geologia Applicata, 1, 157–165.

Ferracuti, L., Marinelli, G., & Rusi, S. (2006). Idrogeologia e monitoraggio delle sorgenti carsiche del Tavo (massiccio carbonatico del Gran Sasso) e loro implicazioni nella gestione dell’ emergenza torbidità. Giornale Di Geologia, 3, 47–52.

Rusi,S., Marinelli, G., Palmucci, W. (2016). La gestione dell’emergenza torbidità delle sorgenti carsiche del Tavo (Appennino Centrale). Atti del Convegno Nazionale “La ricerca carsologica in Italia”, 22-23 giugno 2013, 155-159.

Schnegg, P. (2002). An inexpensive field fluorometer for hydrogeological tracer test with three tracers and turbidity measurement. Proc 32nd and 6th ALHSUD Congress on Groundwater and human development, 21-25 October 2002, 1484-1488.

Tallini, M., Parisse, B., Petitta, M., & Spizzico, M. (2013). Long-term spatio-temporal hydrochemical and 222Rn tracing to investigate groundwater flow and water–rock interaction in the Gran Sasso (central Italy) carbonate aquifer. Hydrogeology Journal, 21(7), 1447–1467.

3 Ubrique test site (case study Spain)

3.1 Introduction

The area selected for Early Warning System (EWS) development and implementation is Ubrique test site, a binary karst area of 26 km^2 in the NE of Cádiz province (S Spain; Fig. 3.1). In this area, mean annual precipitation has been estimated around 1350 mm (the wet season is mainly in winter) and the relief presents an alignment NE-SW with steep slopes that range from 800 to 1400 m.a.s.l. (Sánchez et al., 2017; Marín et al., 2020). Ubrique test site is characterized by Triassic evaporites with clays, Jurassic dolostones (lower) and limestones (upper) -500 meters thick-, and Cretaceous-Paleogene marly-limestones (Martín-Algarra, 1987). The geological structure is defined by anticline folds and synclines matching with depressions constituted by younger marly-limestones materials.

Ubrique test site constitutes a fractured and highly karstified aquifer system where the main outlets are Cornicabra (349 m a.s.l.) (Fig. 3.2a) and Algarrobal springs (317 m a.s.l.) (Fig. 3.2b) (Martín-Rodriguez et al., 2016). Those discharge points are located in the western border of the system between the permeable carbonate rocks and the impervious layers (mainly Cretaceous-Paleogene marly-limestones). Recharge is mainly produced in two ways, (1) diffuse infiltration from rainfall through carbonate outcrops and (2) concentrate flow from small endorheic areas. The most important one is the flysch developed catchment which enters the system through the Villaluenga shaft.

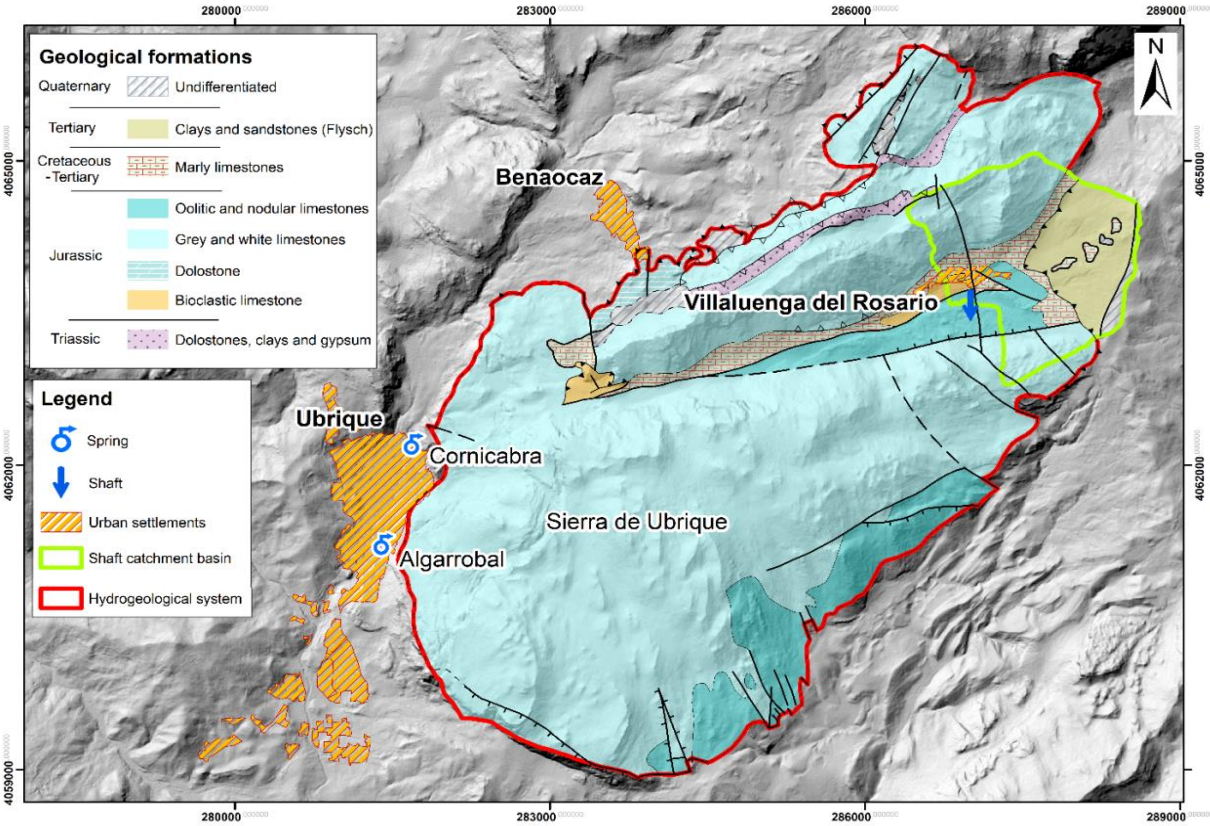

Figure 3.1: Location and hydrogeological setting of Ubrique test site.

After heavy rain episodes, high turbidity values are observed in the springs (Fig 3.2), and thus, the exploitation of spring discharge is unfeasible according to the Spanish law (RD140/2003). The different rural activities (livestock, cheese manufacturing) developed in the recharge area and the spill of the wastewater treatment plant of Villaluenga del Rosario village act as sources of organic contamination, further aggravating the problem caused by turbidity.

Given that drinking water supply is produced only by capturing spring discharge, a great dependence on groundwater is thus generated for the 17.000 inhabitants of Ubrique village.

Figure 3.2: a) Cornicabra and b) Algarrobal springs during high turbidity episode.

3.2 Equipment and methods

A complete monitoring network was established over the recharge area and the two main discharge points in order to control input and output variables of the system. The monitored parameters and related measurement devices are described in Table 3.1. The use of natural fluorescence techniques highlights due to its advantages regarding the quick detection of the arrival of a potential contaminant. Hence, in this study, the use of a field fluorimeter with a specific optic for Tryptophan -Like-Fluorescence (TLF) has been selected due to its apparently good correlation with bacterial activity (Determann et al., 1998; Cumberland et al., 2012; Quiers et al., 2014; Sorensen et al., 2015, 2016; Frank et al., 2018 and Nowicki et al., 2019).

Table 3.1: Early Warning Parameters and related devices used for the monitoring network.

Parameter	Equipment	Method	Resolution	Monitoring frequency
Rainfall	Weather station (Davis Instruments)	Rainfall meter of tipping bucket type	±0.1 mm	1 hour
Flow	Odyssey (Dataflow Systems LTD)	Piezoresistive wire	±0.8 mm	15 min
Temperature	GGUN FL30 (Albilia) HOBO U24 (Onset)	Thermocouple thermometer	±0.1 °C	
Electrical conductivity	GGUN FL30 (Albilia) HOBO U24 (Onset)	Two electrode probe	±1 µS/cm	
Turbidity	GGUN FL30 (Albilia)	Fluorescence	±0.01 NTU	
TLF	GGUN FL30 (Albilia)	Fluorescence	±0.01 ppb	

Furthermore, complementary laboratory analysis were realized in order to complete the database during flooding events and better characterize the occurrence of contamination events. The determined parameters are described in Table 3.2, among which the use of the semi-quantitative method Colisure (Idexx) stands out for the estimation of faecal indicators such as Total coliforms and E. coli.

*Table 3.2: Complementary parameters analysed for EWS development. (*LW: Low Water conditions; ** High Water conditions).*

Parameter	Equipment	Method	Resolution	Monitoring frequency
Major ions	881 Compact IC pro and 792 Basic IC (Metrohm)	Ion chromatography	±0.01 mg/l	Weekly (LW*) 4 hours (HW**)
Total alkalinity	888 Titrando (Metrohm)	Acid-base titration	±0.01 mg/l	
TOC	TOC-VCSN (Shimadzu)	Combustion Catalytic Oxidation	±0.01 mg/l	
Trace metals	ICAP- RQ (Thermo Fisher)	Mass spectrometry	± 0.1 ppb	
Bacteria	Colisure (IDEXX)	Most Probable Number	± 0.1 CFU	
Natural fluorescence	LS-55 (Perkin Elmer)	Fluorescence	± 1 ppb	

In order to reinforce the interpretations of the temporal evolutions of the set of natural responses, a multivariate statistical analysis of principal components (PCA) has been carried out, this method being widely applied in hydrogeological investigations (Bakalowicz, 1979; Mudry and Blavoux, 1986). In this study, PCA has been used in order to better define potential correlations between the different measured parameters: TLF, total coliforms, E. coli, EC, turbidity, TOC, Total N, Al and Mn. Those evaluations have been realized with 25 groundwater samples from each spring from which complete analytical determinations are available. Statistical analyses have been realized with a specific Excel (Microsoft Office) complement XLSTAT Trial Version 2014.5.03 (ADDINSOFT).

3.3 Results and discussion

Four flooding events that hindered the total exploitation of groundwater were registered during hydrological year 2020/21 in both springs of Ubrique test site. Time series of key EWS parameters in Cornicabra spring are shown in Figure 3.3 in which the maximum discharge values between 1200-1800 l/s are observed after a recharge event and the total time span of the flooding events is approximately one week. During that interval, clear dilution processes are observed in the decrease of EC record (periods below 280 µS/cm) together with a decrease of temperature, which indicate the arrival of fast flows from recently infiltrated rain water.

The arrival of contaminants (mainly organic compounds) and suspended particles (which generate high turbidity records) are usually observed before the decrease of EC previously described. Turbidity in Cornicabra spring shows a maximum up to 60 NTU during the first effective recharge event of the hydrological year and the following events do not exceed 20 NTU. Despite the -relatively- low turbidity values, these remain above 5 NTU (the maximum indicated in the Spanish regulation for drinking water) for approximately one week. Tryptophan-Like-Fluorescence (TLF) at Cornicabra spring displays values that range between 20-40 equivalent ppb and the response times are normally contemporary with turbidity. However, TLF variations are sometimes observed when no effective recharge input exists. Those changes seem to be related to local rain effect since the spring is included within the urban environment of the village. The presence of bacterial indicators (Total coliforms, E. coli) varies on each flooding event and its maximum values between 313-980 CFU for TC and 104-517 CFU for E. Coli. In addition, their maximum values seem to keep a direct correlation with spring discharge at each event.

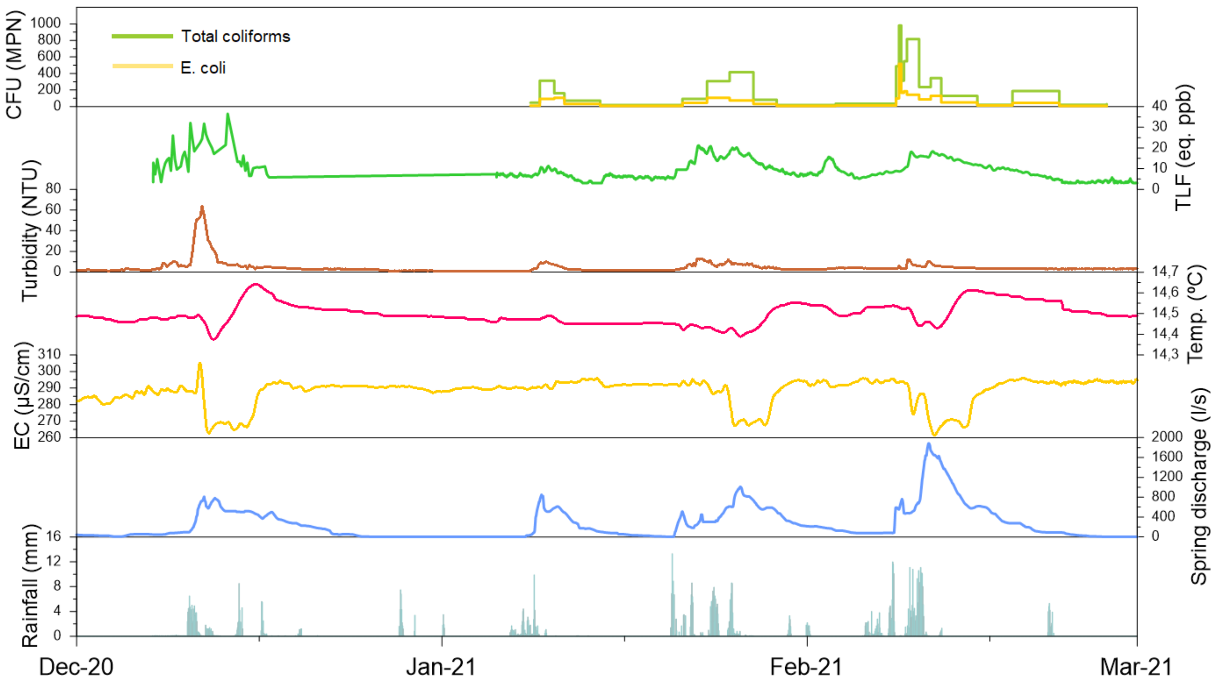

Figure 3.3: Time series of selected EWS parameters in Cornicabra spring between December 2020 and March 2021.

In the same way, time series of key EWS parameters in Algarrobal spring are shown in Figure 3.4, which shows maximum spring discharge close to 800 l/s for the most intense rain events. The records of electrical conductivity and temperature show a different response to that of Cornicabra: the flooding events start with a clear piston effect (increase of EC up to 400 µS/cm) that is only followed by a dilution in two cases (first and last events). Temperature reproduces as well the same shape of EC, rising to 15.6 ºC, which indicates that in this spring the discharge occurs, to a greater extent, from the saturated zone.

The magnitude of the contamination episodes is greater in Algarrobal spring, sediment transport presents a greater importance in this sector of the system, since the maximum turbidity values vary between 200-350 NTU, at least 10 times higher than at Cornicabra spring. Furthermore, just as it happens in Cornicabra, the first effective recharge event produces the maximum turbidity peak. These values can be explained due to the accumulation of sediment in the siphons and conduits of the system during recharge events that do not generate a hydrodynamic response. TLF signal reaches values close to 120 eq. ppb and in some cases, the increase in its concentration occurs before the increase in suspended sediments (turbidity record). Furthermore, the main bacterial indicators reached values close to 3000 CFU at some specific moments.

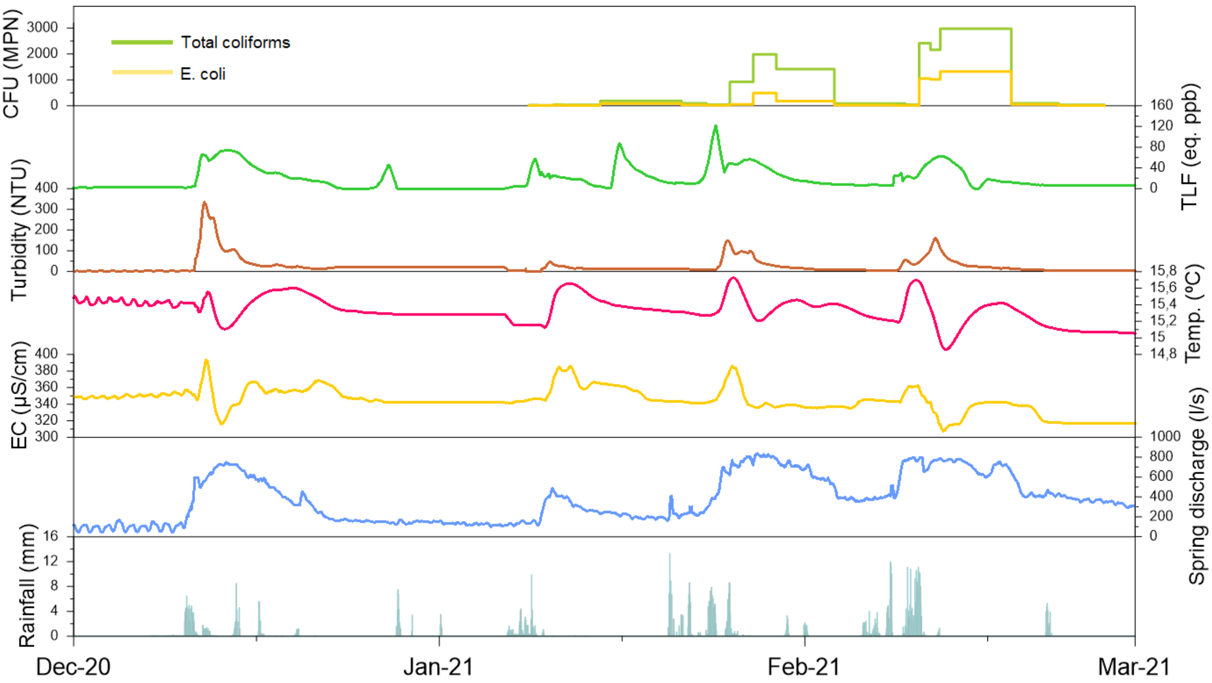

Figure 3.4: Time series of selected EWS parameters in Algarrobal spring between December 2020 and March 2021.

Despite draining the same system, some differences are found in the hydrodynamic behaviour and magnitude of contamination of both springs. For example, Cornicabra spring usually shows spring discharge increase between 12-48 hours before a rain event than Algarrobal spring. This fact might be directly related to the development of karstification and groundwater circulation trough conduits, as Cornicabra spring shows rainfall response thresholds normally much below the case of Algarrobal spring. Furthermore, the impact of contamination is higher in Algarrobal spring due a more developed connection with the Villaluenga shaft, which would explain through greater turbidity and TLF records.

Finally, in order to identify the parameters that show a greater correlation with the indicators of bacterial activity (Total coliforms and E. coli) and other substances that typically indicate low chemical quality or are considered in drinking water national regulation (chloride, sulphate, aluminium), the multivariate statistical analysis has been applied through a Principal Components Analysis. The results are shown in Figure 3.5, in which two groups of parameters are easily identified. The first one, includes the bacterial activity indicators and EWS parameters such as TLF and turbidity together with Al, which is strongly related to sediment transport. In the second group, parameters related to mineralization are found, such as EC, chloride, sulphate and temperature.

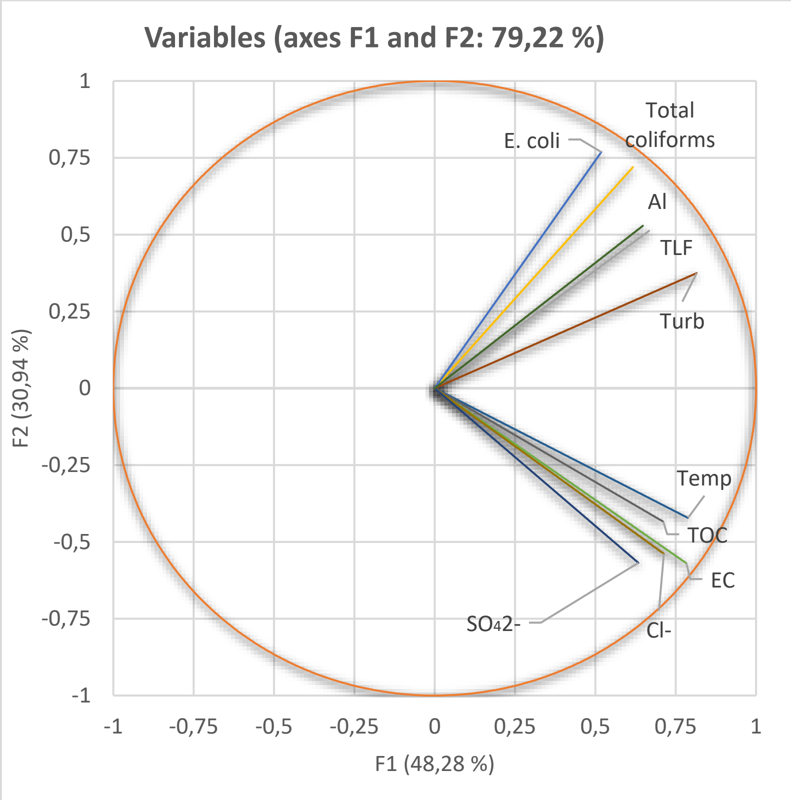

Figure 3.5: Principal Components Analysis results from spring response records at Ubrique test site.

The Pearson correlation matrix extracted from the PCA is shown in Table 3.3. The results show an apparent correlation (p>0.6) of the bacterial activity indicators with parameters such as TLF, turbidity and negative correlation (p<0.1) with mineralization related parameters. This segregation is easily explained depending on recharge magnitude and hydrodynamic conditions. Hence, during an effective recharge event, rainwater rapidly transports bacteria and suspended sediments from the surface to the saturated zone and karst conduits. Thus, when recently infiltrated rainwater with low mineralization and high contaminant load reaches the spring, it produces the decrease of EC due to dilution processes.

Table 3.3: Pearson correlation matrix of main EWS and contamination parameters. Values in bold are different from 0 with a significance level alpha=0,05.

Variables	TLF	Total coliforms	E. coli	EC	Temp	Turbidity	TOC	CL-	SO42-	Al
TLF	**1**									
Total coliforms	**0,733**	**1**								
E. coli	**0,643**	**0,944**	**1**							
EC	0,203	0,083	0,001	**1**						
Temp	**0,309**	0,214	0,113	**0,894**	**1**					
Turbidity	**0,712**	**0,702**	**0,646**	**0,380**	**0,386**	**1**				
TOC	**0,303**	0,117	0,011	**0,852**	**0,862**	**0,339**	**1**			
CL-	0,186	0,065	-0,030	**0,804**	**0,663**	**0,428**	**0,538**	**1**		
SO42-	0,086	0,000	-0,085	**0,759**	**0,564**	**0,387**	**0,462**	**0,926**	**1**	
Al	**0,588**	**0,691**	**0,656**	0,210	0,251	**0,748**	0,222	0,172	0,108	**1**

The information obtained during hydrological year 2020/21 provides a new point of view of this system, since it is the first time that different flooding events have been studied in such detail using novel parameters and methodologies.

3.3.1 EWS workflow and validation

Different precipitation, spring discharge, turbidity and TLF thresholds have been established in order to develop a preliminary workflow for Ubrique test site (Fig. 3.6). This initial scheme includes elements from (1) system input variable (rainfall), (2) system output variable (spring discharge) and (3) variables that represent groundwater quality status (turbidity and TLF). The different alarms have been established using a traffic light-type system, which indicates three warning levels: green – good groundwater quality, yellow – imminent risk of suffering a contamination event, and red – groundwater unfit for human consumption.

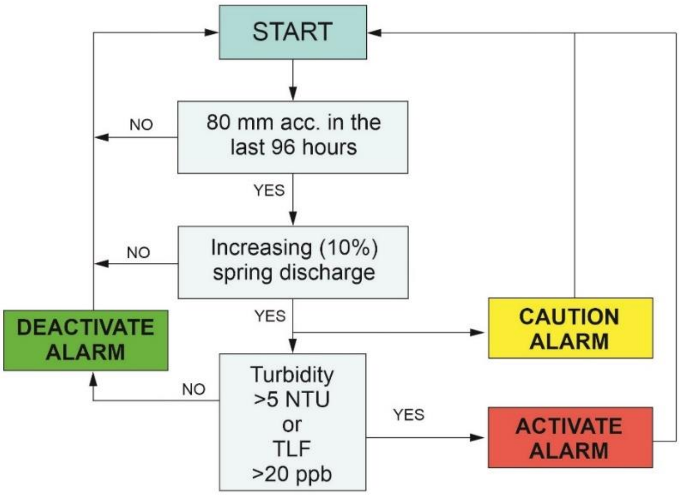

Figure 3.6: EWS workflow developed to control the status of groundwater quality for human consumption.

This workflow has been applied to data series acquired at both springs in the current hydrological year. The case of Cornicabra spring is represented in Figure 3.7 and includes the results obtained between September 2021 and February 2022 when only few events have been recorded.

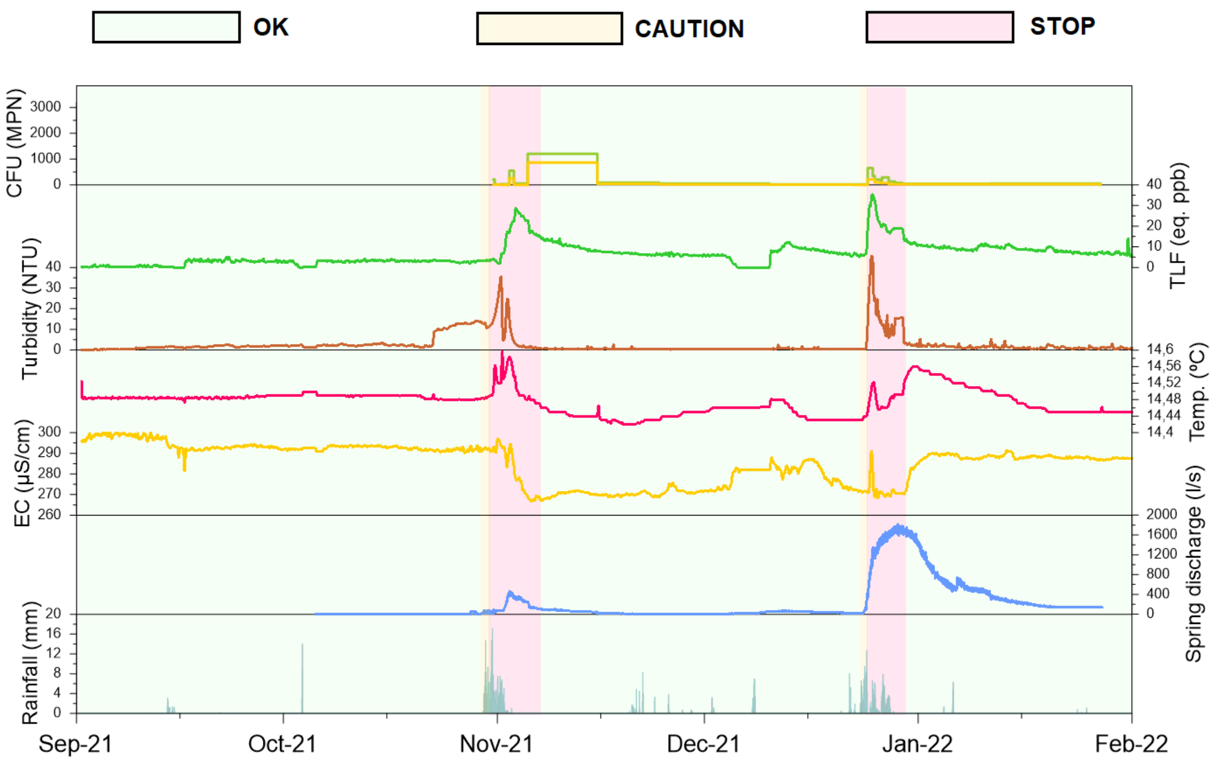

Figure 3.7: Time series of key EWS parameters in Cornicabra spring between September 2021 and February 2022.

At first sight, an anomaly is clearly observed in the first flooding event, since the turbidity record shows how this parameter increases above 10 NTU considerably before the rain event occurs. This false positive is related to the monitoring device characteristics and such turbidity has not been observed until temperature started to rise. Despite that technical incidence, the workflow doesn't send any alert as no rainfall was registered in the previous 48 hours. In this first event, the alert remains active (even though the turbidity is less than 5 NTU), because the TLF signal is greater than 20 ppb and there could still be bacterial activity in the spring. During the second flooding event, the proposed workflow was successfully applied as it perfectly delimits the period in which it would not be convenient to capture groundwater for human consumption.

The same period record at Algarrobal spring is represented in Figure 3.8., where two flooding events after a total accumulated precipitation is 357 mm (first one) and 285 mm (second one) were recorded. However, no spring response -hydrodynamic or hydrochemical- was observed during the first effective recharge event, despite of being the more intense one. This is easily explained due to the initial -really low- soil water content and hydrodynamic conditions in the system after certainly dry summer.

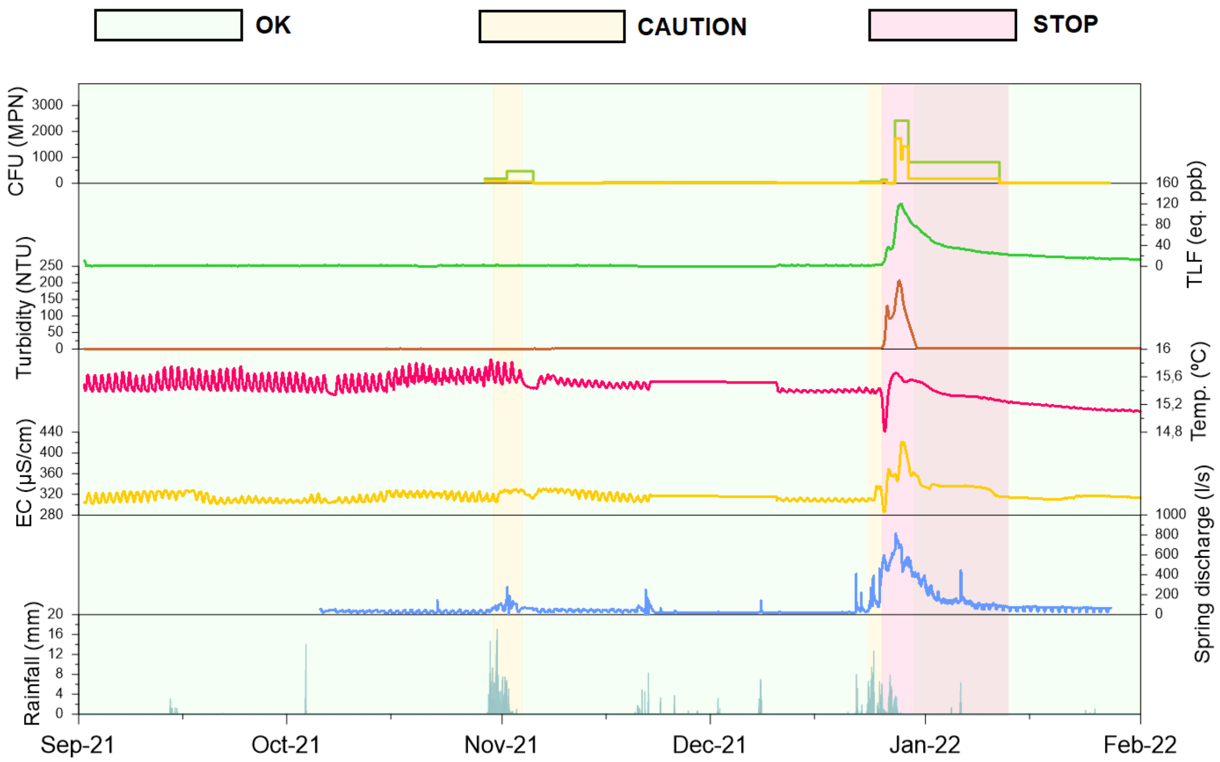

Figure 3.8: Time series of key EWS parameters in Algarrobal spring between September 2021 and February 2022.

As explained before, when no spring response was observed, the workflow mechanism warns about the potential risk of suffering a contamination event due to the high amount of accumulated rainfall. During the second flooding event, the long-tailed TLF curve hinders the total exploitation until TLF decreases under 20 ppb (similar situation to Cornicabra spring). The sustained TLF tail could be due to be a malfunction (lamp issue) of the measurement device, since the recorded signal does not return to the pre-flooding values.

3.4 Conclusion and future steps

The two first phases (continuous record of spring natural responses and statistical analysis) of the implementation of an Early Warning System at Ubrique test site have been successfully accomplished. Furthermore, a preliminary workflow has been developed for identifying the occurrence of contamination episodes based of a combination of precipitation, discharge TLF and turbidity data acquired during the hydrological year 2020/2021. Due to the reduced number of precipitation events during this time, the validation of the proposed workflow has been realized with continuous data records of two flooding events between September 2021 and February 2022. Thus, in order to better test the robustness of the EWS workflow, the validation process should be further developed with successive flooding events.

The selected procedure for continuous monitoring (natural fluorescence methods) constitutes a quick and low budget approach to estimate -near real time- groundwater quality. However, the obtained results and EWS parameters thresholds are still semi-quantitative, as this method shows multiple limitations, such as signal quenching or light intensity variations, which reduce the accuracy of the measurements.

The next step comprises the definitive EWS launching with the implementation of a telemetry system and the introduction of an online server for real-time data visualization, processing and generation of warning alerts.

3.5 References

Bakalowicz M (1979) Contribution de la geochimie des eaux à la connaissance de l'aquifere karstique et de la karstification. (Contribution of water geochemistry to the knowledge of karst aquifer and karst processes). Doctorat es Sciences naturelles Thesis, P. et M. Curie Paris-6, Paris, 269 pp.

Cumberland, S., Bridgeman, J., Baker, A., Sterling, M., Ward, D. (2012) Fluorescence spectroscopy as a tool for determining microbialquality in potable water applications. Environ. Technol. 33, 687–693

Determann, S., Lobbes, J.M., Reuter, R., Rullkotter, J. (1998) Ultraviolet fluorescence excitation and emission spectroscopy of marinealgae and bacteria. Mar. Chem. 62, 137–156

España. Real Decreto-ley 140/2003, de 7 de febrero, por el que se establecen los criterios sanitarios de la calidad del agua de consumo humano. Boletín Oficial del Estado, 21 de febrero de 2003, núm. 45, pp. 7228 a 7245.

Frank S, Goeppert N, Goldscheider N (2018) Fluorescence-based multi-parameter approach to characterize dynamics of organic carbon, faecal bacteria and particles at alpine karst springs, Sci. Total Environ. 615:1446-1459.

Marín, A.I., Martín Rodríguez, J.F., Barberá, J.A., Fernández-Ortega, J., Mudarra, M., Sánchez, D. and Andreo, B. (2021) Groundwater vulnerability to pollution in karst aquifers, considering key challenges and considerations: application to the Ubrique springs in southern Spain. Hydrogeol Journal, 29:379–396.

Martín-Algarra, M. (1987) Evolución geológica alpina del contacto entre las Zonas Internas y Externas de la Cordillera Bética. PhD Thesis, University of Granada, Spain. 1171 p.

Martín-Rodriguez, J.F., Sánchez-García, D., Mudarra-Martínez, M., Andreo-Navarro, B., López-Rodríguez, M., and Navas-Gutiérrez, M.R. (2016) Evaluación de recursos hídricos y balance hidrogeológico en acuíferos kársticos de montaña. Caso de la Sierra de Grazalema (Cádiz, España). Book chapter on Las aguas subterráneas y la planificación hidrológica, 163-170. Spanish-Portuguese Congress. IAH Spanish Chapter. Madrid (Spain), November 2016.

Mudry, J. and Blavoux, B. (1986). Utilisation de l'analyse en composantes principales (sur variables centrées réduites) pour l'étude du fonctionnement hydrocinématique de trois aquifères karstiques du Sud-Est de la France. Hydrogéologie 1, 53–59.

Nowicki, S., Lapworth, D.J., Ward, J.S., Thomson, P., Charles, K., 2019. Tryptophan-like fluorescence as a measure of microbial contamination risk in groundwater. Sci. Total Environ. 646, 782–791.

Quiers M, Batiot-Guilhe C, Bicalho CC (2014) Characterisation of rapid infiltration flows and vulnerability in a karst aquifer using a decomposed fluorescence signal of dissolved organic matter. Environ Earth Sci 71(2):553–561.

Sánchez, D., Barberá, J.A., Mudarra, M. and Andreo, B. (2017). Hydrogeochemical tools applied to the study of carbonate aquifers: examples from some karst systems of southern Spain. Environmental Earth Sciences, 74, 199–215.

Sánchez, D., Martín-Rodríguez, J.F., Mudarra, M., Andreo, B., López, M. and Navas, M.R. (2016). Time-lag analysis of natural responses during unitary recharge events to assess the functioning of carbonate aquifers in Sierra de Grazalema Natural Park (Southern Spain). Eurokarst 2016, Neuchâtel, pp 157- 167, ISBN:978-3-319-45465-8.

Sorensen, J., Lapworth, D., Marchant, B., Nkhuwa, D., Pedley, S., Stuart, M., Bell, R., Chirwa, M., Kabika, J., Liemisa, M. (2015). In-situ tryptophan-like fluorescence: a real-time indicator of faecal contamination in drinking water supplies. Water Res. 81, 38–46.

Sorensen, J., Sadhu, A., Sampath, G., Sugden, S., Gupta, S.D., Lapworth, D., Marchant, B., Pedley, S. (2016) Are sanitation interventions a threat to drinking water supplies in rural India? An application of tryptophan-like fluorescence. Water Res. 88, 923–932.

4 The Lez Karst Catchment (case study France)

4.1 General description of the EWS developed

The Mediterranean Lez basin is a large karst system (L-KS) located north of Montpellier, south-east of France (Figure 4.1). The Lez aquifer system, located in the Garrigues karst area, is roughly bounded by the Hérault and Vidourle rivers (western and eastern sides), and the Cevennes and Nimes faults (northern and southern sides) (Figure 4.1). The elevation ranges from 15 m.a.s.l (Vidourle's banks) to 658 m.a.s.l (Saint-Loup mountain). While the northern area of the L-KS is little urbanized, the south-eastern area is characterized by an increased urbanization.

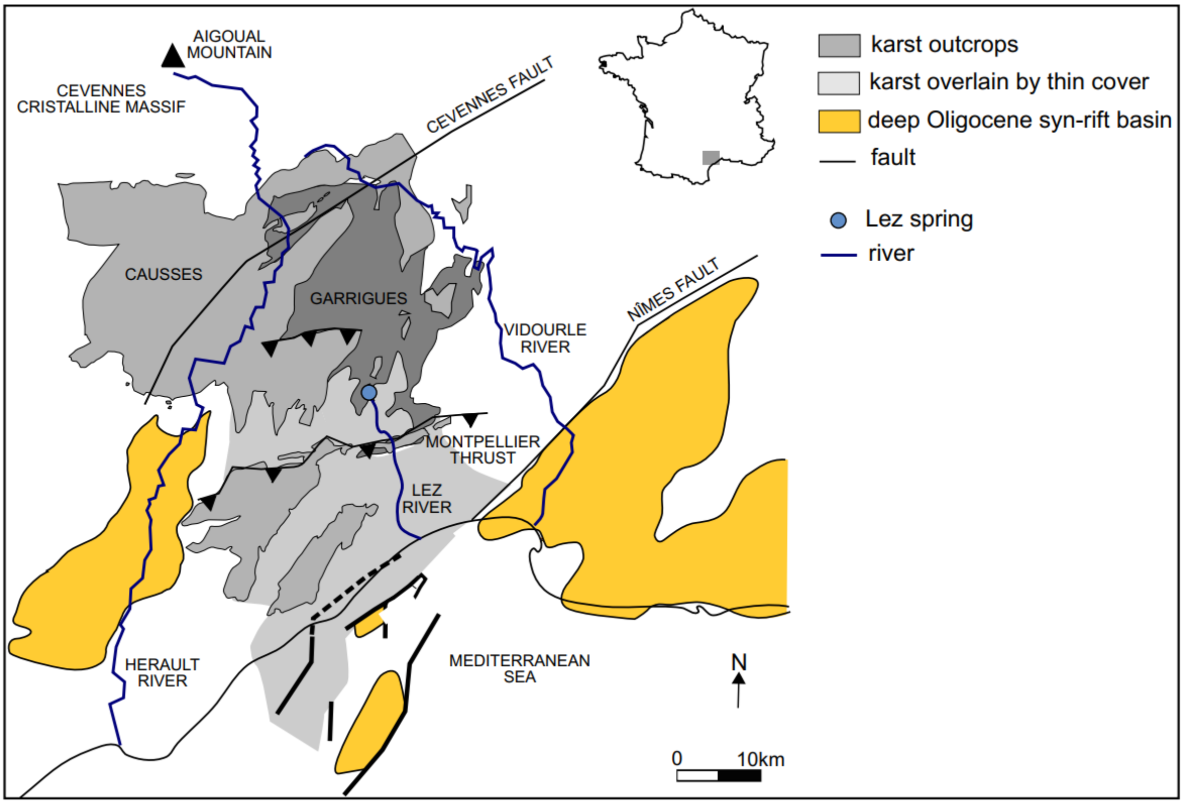

Figure 4.1. (A) Geographical location and boundaries of the Lez karst system (L-KS) (from Mazzilli, 2011, simplified after Camus, 1999).

The Lez aquifer integrates Upper Jurassic and Early Cretaceous limestones, overlain by Callovian–Oxfordian marls and locally covered by a thick succession of Early Valanginian marls and marly limestone. These sedimentary layers are highly and deeply karstified (Leonardi et al., 2011) due to the Messinian salinity crisis (about 5.5 My ago) when the sea-level of the Mediterranean Sea descended more than 1000 m (Audra et al., 2004; Clauzon et al., 2005). The aquifer is divided by NE-SW normal faults associated with the Pyrenean orogeny (Eocene) and subsequently impacted by the Oligocene extension period. In consequence, the Lez aquifer is mainly unconfined to the southwest, while it is mainly confined to the northeast. The soils are characteristic of karst systems, either non-existent or shallow and poorly developed. Some low scrublands and woods, adapted to drought, cover these soils. Agriculture is mostly represented by the vineyards.

A Mediterranean climate characterizes L-KS, with dry summers and rainy autumns. The temperatures are warmer in summer (mean temperature ~ 22 °C) and slightly cooler in winter (mean temperature ~ 5 °C). The rainfall decrease from south to north because of the ascending topography and the closeness of the Cevennes massif (Figure 4.1). Rainfall is highly variable ranging from dry (600 mm.yr-1) to wet years (1200 mm.yr-1) basis. The annual rainfall regime is bimodal, with a stronger peak from September to December and a weaker peak from March to May. The annual recharge occurs with the first intense rainfall events in autumn, so-called Cevenols or Mediterranean episodes. During these intense convective rain events, the accumulated daily rainfall can reach several hundreds of mm, e.g. 473 mm recorded at the Ceyrac rain gauge in September 2002.

The major anthropogenic impacts on the water quality of the Lez spring are summarized below:

- Agricultural activities correspond to approximately 25% of the surface area of the basin (Batiot et al., 2013). Vulnerable areas linked to these activities are essentially vineyards. These may explain the excess of the potability standards for phytosanitary products during high flows. Concerning agricultural contamination, regular analyses during a hydrological cycle (September 2010 to September 2011) of 16 pesticides in the waters of the Lez spring indicate a level of very low contamination (<25 ng/l). For some compounds, the concentration variations showed a seasonal use such as herbicides. These results have been compared with those resulting from others punctual samplings at the Lez spring (ADES data, 1997-2011). The average and maximum concentrations observed are generally low (respectively <30 ng/l and 50 ng/l) for all molecules. Punctually, compounds such as simazine or diuron may exceed 100 ng/l. As a result, the Lez aquifer does not appear to be chronically contaminated with pesticides, even if some molecules may exceed the potability standard set at 100 ng/l during flood events.

- In the Lez spring catchment, many areas have low permeable covers of low thickness, or present calcareous outcrops fractured and karstified which induce infiltration of water through the aquifer. Urbanized areas represent about 5% of the basin. As other Mediterranean areas, the population of the basin doubled between 1990 and today. Wastewaters of the cities located in the southern part of the basin are collected and treated by the regional treatment plant of MAERA. In the northern part of the basin, urbanization has increased significantly in some areas, but the infrastructure to treat urban or domestic wastewater is not sufficient. Thus, peaks in bacterial pathogen content can be measured at the Lez spring during flood events or very dry conditions. The more vulnerable areas for water quality are sink-holes located in temporary streams where concentrated infiltration occurs during flood periods. Moreover, some are located near wastewater treatment plants which discharge effluents in these temporary streams, without dilution of the residual nutriments or bacterial contaminants after treatment. Due to their specific location around the major fault zone of Corconne-Les Matelles, the pollution is easily transported by subterranean flows to the Lez spring.

The Lez aquifer supplies drinking water to ~ 350 000 inhabitants of Montpellier metropolitan area. The pumping station, located within the karst conduit at a depth under the level of the Lez spring outlet (65 m.a.s.l), provides about 30 to 35 Mm3 of water per year (mean annual pumping flow rate of 1020 L.s-1 between 2008 and 2020). Pumping can cause a drop in water level of up to 30 m at the end of the low water period, but the aquifer is fully recharged and its reserves are renewed during autumn and winter. National regulations allow pumping at a higher rate than natural discharge of this Vauclusian-type spring (mean discharge ~ 2200 L.s-1), if a minimum discharge (~ 230 L.s-1) is respected to ensure the ecological functions of the watercourse and reduce hazards flood by storing rainfall in autumn (Avias, 1995, Jourde et al., 2014). The water quality of the Lez spring is affected by bacteriological contaminations because of the infiltration of (not)treated wastewaters, mainly during flood events. Prior to distribution, the pumped water is treated at the Arago treatment plant, where turbidity is reduced to below 4 NTU by flocculation of suspended particles and then disinfected with chlorine gas.

The main objective is developed Early Warning System (EWS) indicators (Grayman and Males, 2002) to track the origin and type of karst waters. These tools are based on conventional hydrochemical parameters coupled with innovative parameters such as the fluorescence of dissolved organic matter (Stedmon et al., 2011). The fluorescence of humic-like compounds is suitable for monitoring rapid infiltration flows during high-flow periods. Whereas the fluorescence of protein-like compounds provides further information, as it can be used to track fecal bacteria from domestic wastewater pollution.

4.2 Equipment and methods used

The monitoring at the Lez karst system (L-KS) is carried out by the MEDYCYSS Observatory (OSU OREME, OZCAR-THEIA, DEIMS-SDR eLTER) since 2006 and encompasses the following data:

- Hydroclimatic information

Every 15 minutes from 2010, by two meteorological stations, including: precipitation, air temperature, humidity, solar radiation, wind speed and direction. This database is complemented with six rain gauge stations (from 2006) distributed over the system to estimate the temporal and spatial rainfall distribution.

- In situ monitoring

Water level (every 15 minutes from 2007), natural organic matter (GGUN FL918: field fluorimeter: Humic NOM, proteic NOM and turbidity every 15 minutes from 2015), physico-chemical (YSI6920 V2-2-SV probe: **water temperature, electrical conductivity**, pH, **turbidity, dissolved oxygen** and chlorides; every hour from 2015), Radon-222 (RAD7 Durridge™ : ^{222}Rn , every hour only during Molina-Porras PhD Thesis, 2016-2017), and other parameters (Spectro::lyser 3 s::can probe : Turbidity, UV 254, TOC, DOC, **NO_3** every 15 minutes from March 2021), continuously recorded at the perennial Lez spring (Figure 4.2).

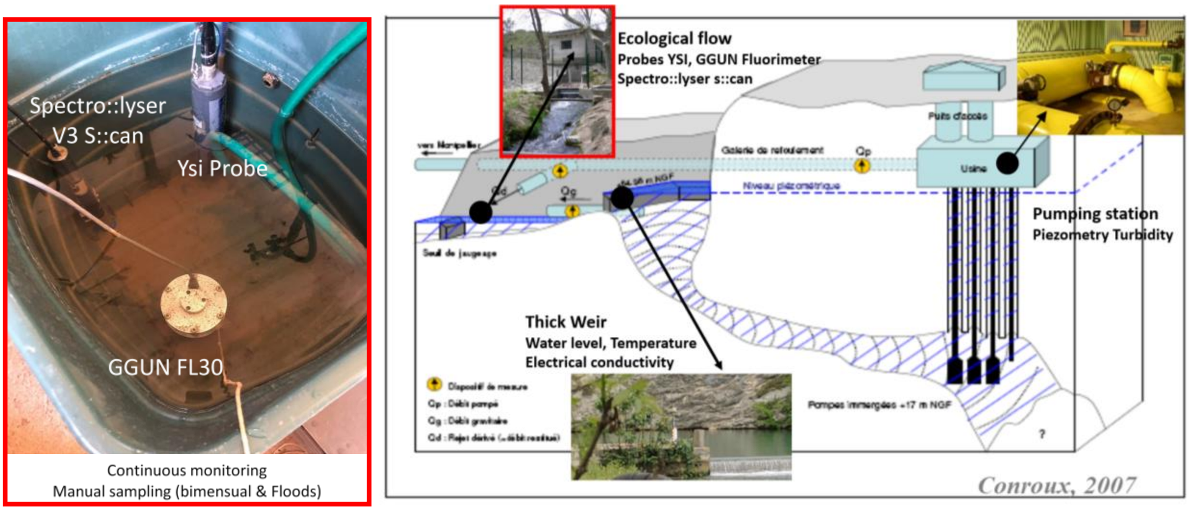

Figure 4.2: Monitoring at Lez spring (weir), upstream (pumping station) and downstream (ecological flow).

- Regular sampling

Physico-chemical parameters and water samples are carried out every two weeks and with a shorter time span during flood events since 2006. The chemical (major elements, TOC, NOM, trace elements), isotope (water stable isotopes) dissolved gaz (^{222}Rn) and bacterial (Total coliforms and E. Coli) analyses are performed at HydroSciences Montpellier laboratory of the University of Montpellier, France (except for trace elements, see after).

At the same time, T, pH and EC (Tref=25°C) were measured in the field using a portable pH meter and conductivity meter (WTW 3210 i). Except for trace elements, analyses are performed at HydroSciences Montpellier laboratory of the University of Montpellier, France.

Sampling for major and trace element determination was realized in acid washed HDPE bottles, filtered on-site with disposable PP syringe and Durapore membrane (0.22 µm) and stored in acid washed HDPE bottles. Aliquots for cations and trace elements were acidified with ultrapure HNO3 (1‰ v/v). Water for TOC and for NOM analyses were sampled in pre-cleaned and combusted 60 mL amber glass bottles. All samples were stored at 4°C before analysis. Chemical analyses were performed at the HSM water chemistry laboratory. Total alkalinity was measured by acid titration with HCl 0,1N (Gran method) within one day. Major ions (Cl- , NO3- , SO42- , Ca2+, Mg2+, Na+ , and K+) were analyzed by ion chromatography (ICS 1000 Dionex®). Precision error was < ± 5%. Trace elements (Li, B, Al, Si, Ti, V, Cr, Mn, Fe, Co, Ni, Cu, Zn, As, Rb, Sr, Mo, Cd, Cs, Ba, REE, Pb, and U) were analyzed with Q-ICPMS (iCAP Q, Thermo Scientific®) after acidification at 1% HNO3 v/v at the AETE-ISO (Analyse des Elements en Trace dans l'Environnement et Isotopes) technical platform of the OSU OREME, University of Montpellier. Precision error was typically < ± 8%. River water reference material for trace metals SLRS-6 (National Research Council, Canada) was analyzed every 20 samples to check analysis accuracy. Mean results were within the range of certified uncertainties. Total Organic Carbon (TOC) was measured after acidification with H3PO4 (1‰ v/v) on a carbon analyzer SHIMADZU™ TOC-VCSH (catalytic combustion method). The NOM fluorescence analyses were carried out usually within 48 h after the sampling. The fluorescence spectra were recorded using a SHIMADZU™ RF-5301 PC (xenon lamp) 3D spectrometer. Determination of 222Rn activity in water was conducted in the laboratory using an Alphaguard PQ 2000 device (GENITRON™ Instruments GmbH) equipped with the Aquakit system with a precision < 10%

Water stable isotopes (δ18O and δD) are analyzed at the mass spectrometry laboratory of HydroSciences Montpellier on an Isoprime mass spectrometer. δ18O is measured with the classical CO2 equilibration method, with an overall uncertainty of ± 0.1‰. δD is measured in continuous-flow mode with an Eurovector Pyr-OH analyzer converting H2O to H2 on Cr at 1070 °C, with an overall uncertainty of ± 0.8‰. All isotopic water values are reported relative to the V-SMOW scale.

The parameters in bold are suggested to be used as EWS indicators to put in evidence fast infiltration within the aquifer and potential pollutions. Chloride may be relevant to monitor the contribution of waters coming from deeper compartments.

4.3 Results and discussion

The study of karst springs is complex due to their high reactivity to flood events. To better characterize the Lez aquifer functioning, regular and flood events water samplings need to be completed by in situ monitoring with high frequency measurements (Figure 4.3).

A clear seasonality is observed with increasing rainfall events, piezometric level (NP) and discharge coupled with decreasing water temperature in winter. While the opposite pattern is observed in summer. A nictemeral behaviour is noticed with water temperature and discharge. The first is related to day-night variation and the latter to daily water pumping. Water pumping also affects the drop of NP in summer, increasing the rate of decline. The NP is highly reactive to the Cévennes rainfall events that occur at the beginning of the hydrological year (September).

The variations in physico-chemical, chemical and bacterial parameters respond mainly to hydrological variations.

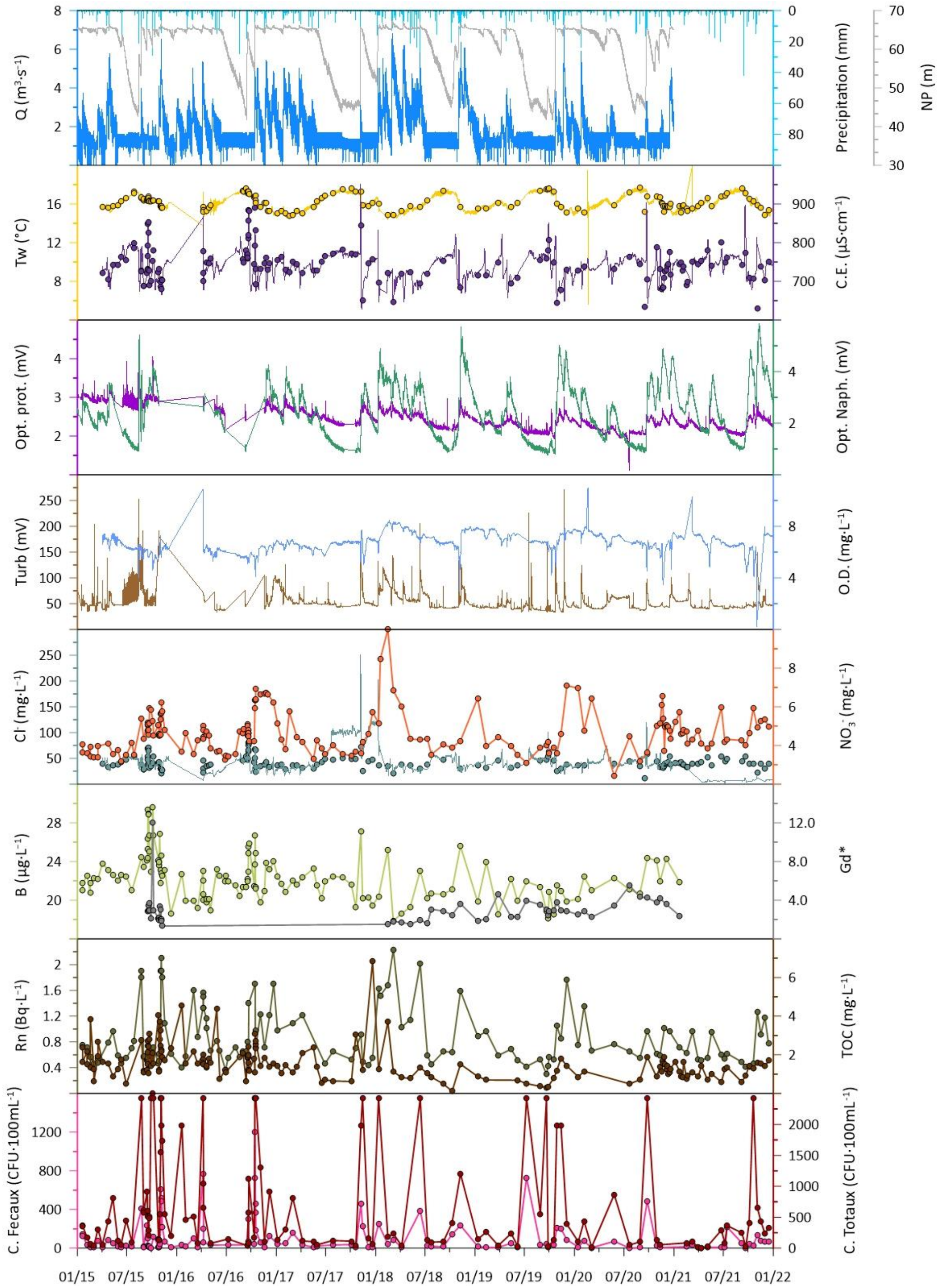

Figure 4.3: High frequency temporal series of the stream discharge (Q), rainfall (P), piezometric level (NP), physicochemical (water temperature (water T), conductivity (Cond), turbidity (Turb), dissolved oxygen (OD) and Chlorides (Cl-)), natural organic matter (humic and proteic fluorescence signal) since 2015. Dots represent punctual streamwater sampling during the study period (N = 52-166) of chemical (Nitrates (NO3-), TOC, Rn, B and Gd) and biological (Total coliforms and E. Coli) parameters.*

The Lez spring is characterized by a complex mixing of mineralized waters with long residence times which derive from Jurassic (1) and deeper aquifers (2), and recently infiltrated waters less mineralized (3), may affected by anthropogenic contaminants (4) (Bicalho et al., 2012).

The different source of the waters at the Lez spring were identified using statistical analyses (Figure 4.4):

(1) Superficial circulation within the main aquifer (Upper Jurassic and Cretaceous limestones). These waters are characterized by a strong signal from the carbonate dissolution products, i.e., Ca^{2+} and HCO_3^-. These two elements are the main ions of the water chemistry in carbonate karst systems. Consequently, the conductivity is strongly influenced by this water source;

(2) Water coming from deep circulation within Middle Jurassic and deeper compartments (Trias and/or Paleozoic) which can move up thanks to the major regional fault of Corconne-Les Matelles. These waters are distinguished by a strong signal of chlorides (Cl^-), magnesium (Mg^{2+}) and sulphate (SO_4^{2-});

(3) Surface-water interactions and interactions with the marls of the Valanginian cover of the aquifer. These waters represent rapid surface infiltration into the aquifer and surface runoff. The interaction with the soils is therefore high, increasing the concentration of TOC and Rn;

(4) Surface waters polluted by anthropogenic effluents. These waters, mainly impacted by sewage, show a high concentration of total and fecal coliforms.

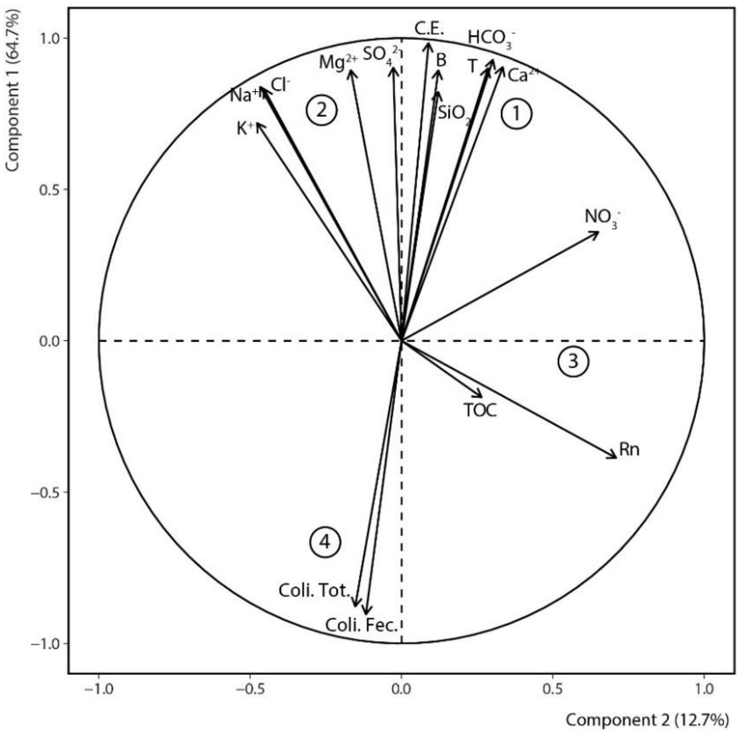

Figure 4.4: Principal component analysis (PCA) of the main physico-chemical, chemical and biological parameters measured at the Lez spring for the period 2012–2020 (N = 143).

The proportions of these different water types vary during the hydrological cycle and depend on the hydrodynamical condition of the aquifer. Previous studies showed that Lez spring waters have a good chemical quality even if they can be affected by punctual contaminations during flood events or very dry periods and may show peaks for fecal bacteria at these periods.

Fast infiltration and pollution fluxes can be highlighted at the Lez spring by a decrease of electrical conductivity, water temperature and dissolved oxygen, and increase in natural fluorescence (red vertical line, Figure 4.5) as well as bacterial compounds and TOC. The natural fluorescence allows to measure humic-like (pedogenic origin) and proteic-like (anthropogenic origin, Quiers et al., 2014, Frank et al., 2018) compounds. Therefore, the proteic signal highlights pollution peaks related to wastewater pollution.

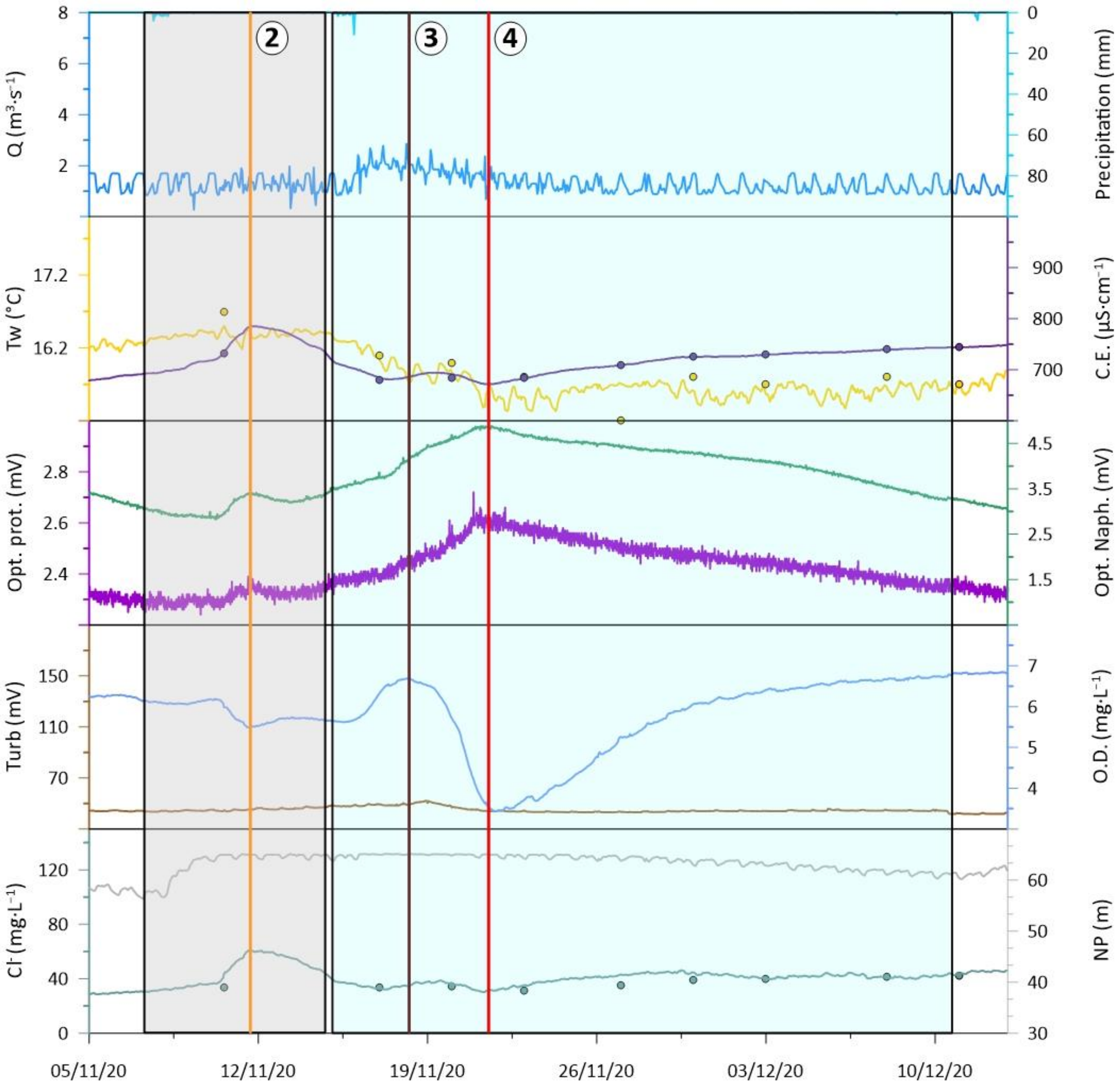

Figure 4.5: Hydrograph and chemograph during two successive hydrological events (grey and cyan surfaces). The colors of vertical lines represent the main source of these waters: deeper aquifers (2, orange), recently infiltrated waters (3, brown) and anthropogenic contaminants (4, red).

This increase can be accompanied by an increase of Boron, Gadolinium anomaly, faecal coliforms and, as well as a strong decreased in dissolved oxygen (O.D.), which are typical indicators of a punctual contamination by waste-waters infiltration within the aquifer. The dissolved oxygen decreases due to higher oxidation rates of organic matter from wastewater effluent in the river (Equation 4.1).

$$CH_2O + O_2 \rightarrow H_2O + CO_2 \tag{4.1}$$

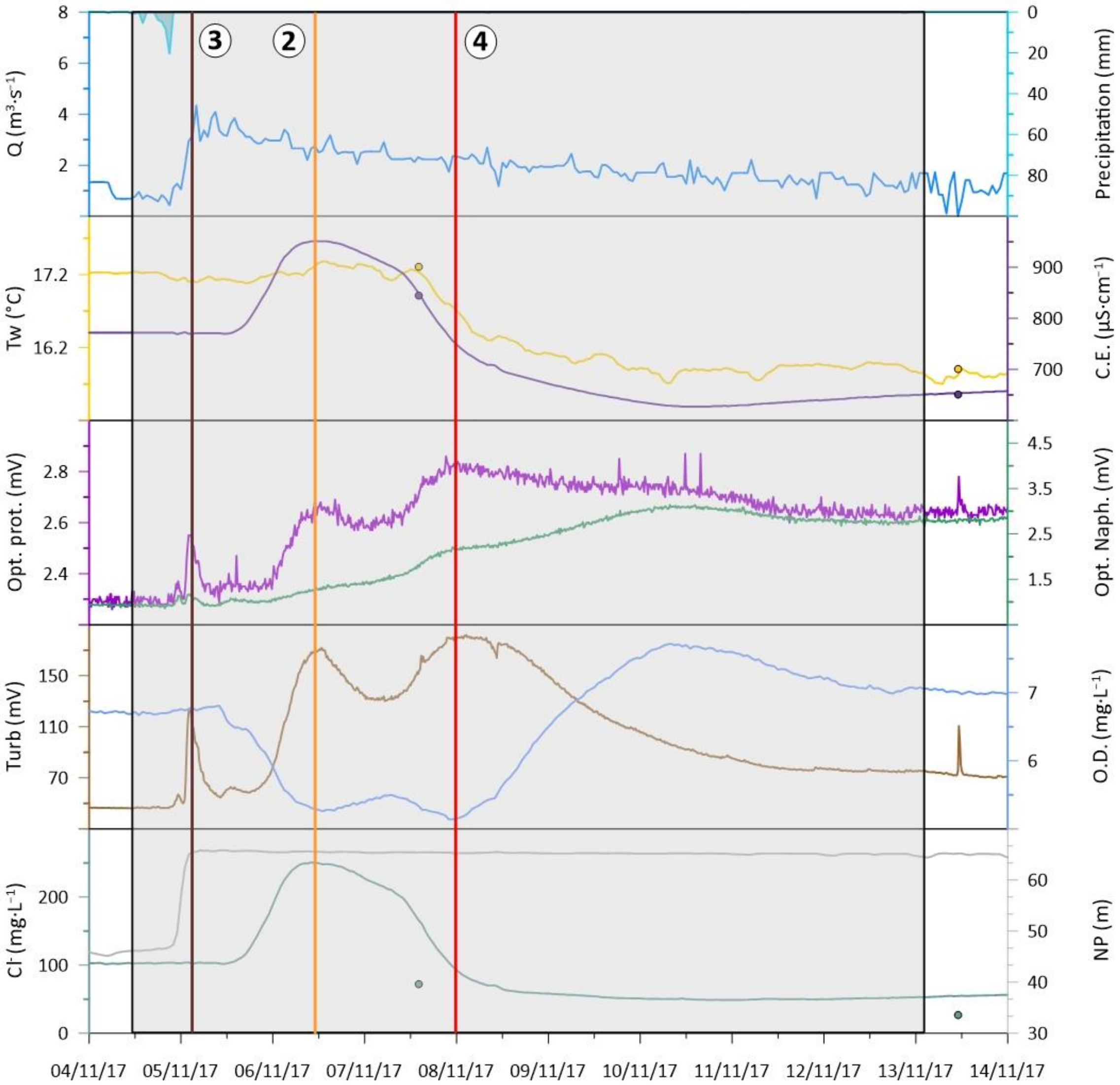

Figure 4.6. Hydrograph and chemograph during one hydrological event (grey surfaces). The colors of vertical lines represent the main source of these waters: deeper aquifers (2, orange), recently infiltrated waters (3, brown) and anthropogenic contaminants (4, red).

A constant discharge does not always indicate a constant water quality (Frank et al., 2018). At the Lez spring, the effect of pollution on water chemistry is observed when there is little or no hydrological variation. During the first hydrological event (grey surface, Figure 4.5), except for the daily discharge variation due to pumping station, only the piezometric level increases. This increase is accompanied by an increase in conductivity and chloride concentration, coupled with a decrease in dissolved oxygen (yellow vertical line, Figure 4.5). All these variations indicate an important contribution of the deeper compartments to the water signal. The second hydrological event (cyan surface, Figure 4.5) shows a slight increase in discharge due to a small rain event. Water temperature and conductivity decrease, while the humic and protein fluorescence signal increases. However, dissolved oxygen shows two different behaviours, first increasing (brown vertical line, Figure 4.5) and then decreasing (red vertical line, Figure 4.5). The first part characterises a rapid contribution of natural infiltration, while the second part shows a contribution of polluted waters. These behaviours were again observed during flooding events (Figure 4.6) coupled to high values of faecal coliform (461 CFU/100mL), reaffirming the usefulness of these parameters for the identification of water sources in the karst systems.

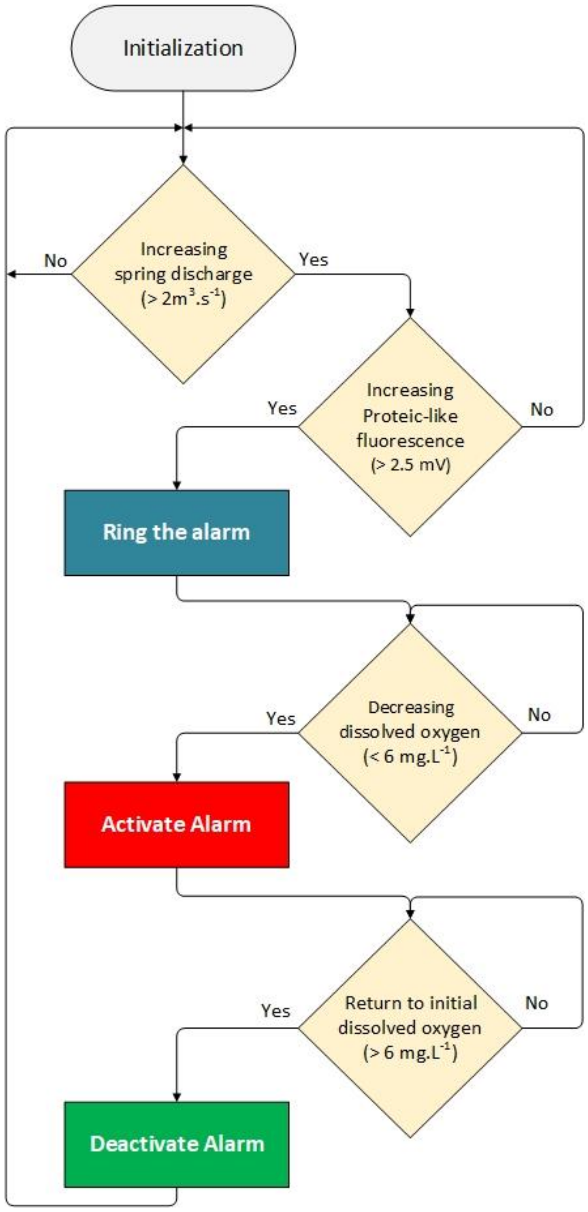

Figure 4.7. Workflow of early warning system (EWS) indicators of anthropogenic pollution in the Lez karst spring.

After identifying the key parameters of the EWS, we developed a simple workflow adapted to Lez spring, based on rate variation of spring discharge, proteic-like fluorescence and dissolved oxygen (Figure 4.7). For example, the application of this method to the Lez spring during 2020 led us to identify three potential episodes of anthropogenic pollution with a duration of 10 days (20/11-29/11), 4 days (22/09-25/09) and 3 days (21/12-23/12) (Figure 4.8). The highest value of faecal coliform (488 CFU/100mL, other values were lower than 73 CFU/100mL) was observed during the first pollution event identified (24/09). However, faecal coliform data from mi-November to December are not available to confirm the other two pollution episodes. Due to its flexibility, this method could be used for other systems, adapting the key EWS indicators.

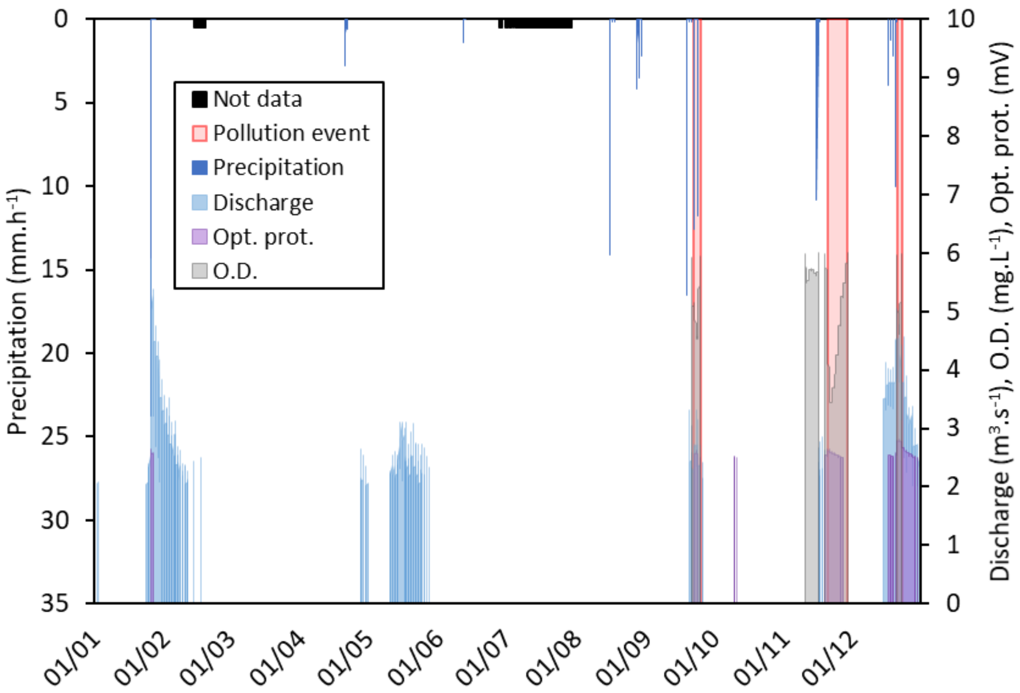

Figure 4.8. Application of early warning system (EWS) indicators to the Lez karst spring in 2020. The red surface indicated a potential anthropogenic pollution.

Some potentially interesting parameters have not been taken into account. Turbidity in the spring water can be either originated from autochthonous (remobilization of sediments inside the karst aquifer) or allochthonous (sinking stream and land surface) (Pronk et al., 2007). Autochthonous suspended particles are mainly observed during floods in non-anthropized karst systems (Ulloa et al., 2021). However, allochthonous turbidity from sewage pollution in the Lez spring is low and generally masked by the autochthonous turbidity, which precludes its use as an indicator of EWS.

4.4 Conclusions

In the case of the Lez spring, we could monitor the influence of the more mineralised waters coming from deep compartments by continuous measurements of Chloride. Fast infiltration associated or not with punctual pollution was evidenced with TOC, NO3- and natural fluorescence in situ monitoring, allowing highlight pollution within the system and to specify its origin (wastewaters impacts for example). In addition, in-situ parameters used to monitor water quality, such as turbidity, are not sufficient to indicate if there is an effective pollution or not linked to the recharge fluxes. The fluorescence monitoring of NOM with hydrochemical analysis was a complete set of tools to characterise the recharge and the vulnerability of complex karst systems.

4.5 References

Avias J. V., 1995. Gestion active de l'exsurgence karstique de la source du lez, Hérault, France, 1957-1994. Hydrogéologie (Orléans) 1995: 113-127

Audra P.H., Mocochain l., Camus H., Gilli E., Clauzon, G., Bigot J.Y., 2004. The effect of the Messinian deep stage on karst development around the mediterranean sea. examples from southern France. Geodinamica acta, 17/6, 27–38.

Batiot-Guilhe, C., Ladouche, B., Seidel, J.-L., Maréchal, J.-C., 2013. Caractérisation hydrochimique et qualité des eaux de l'aquifère karstique du lez (SE de la France). Karstologia 62, 23-32.

Bicalho C.C., Batiot-Guilhe C., Seidel J. L., Van Exter S., Jourde H., 2012. Hydrodynamical changes and their consequences on groundwater hydrochemistry induced by three decades of intense exploitation in a Mediterranean Karst system. Environmental Earth Sciences, Volume 65, Issue 8, 2311-2319.

Clauzon G., Suc J.-P., Popescu S.-M., Marunteanu M., Rubino J.-L., Marinescu F. and Melinte M.-C., 2005. Influence of mediterranean sea-level changes on the Dacic basin (Eastern Paratethys) during the late Neogene; the mediterranean Lago mare facies deciphered. Basin Research 17: 437-462.

Frank, S., Goeppert, N., Goldscheider, N., 2018. Fluorescence-based multi-parameter approach to characterize dynamics of organic carbon, faecal bacteria and particles at alpine karst springs. Science of the Total Environment 615, 1446–1459.

Grayman, W.M., Males, R.M., 2002. Risk-based modelling of early warning systems for pollution accidents. Water Science and Technology 46, 41–49.

Jourde H., Lafare A., Mazzilli N., Belaud G., Neppel L., Dörfliger N. and Cernesson F., 2014. Flash flood mitigation as a positive consequence of anthropogenic forcing on the groundwater resource in a karst catchment. environmental earth sciences: 1-11.

Leonardi, V., Tissier, G., Jourde, H., 2011. Eléments de genèse des karsts péri-méditerranéens: impact de la tectonique sur l'évolution des drains karstiques (karsts nord-montpelliérains). In: Proceedings of the 9th Conference on Limestone Hydrogeology. Besancon, France.

Mazzilli N., 2011. Sensitivity and uncertainty associated with the numerical modelling of groundwater flow within karst systems. PhD, Université Montpellier 2, France.

Pronk, M., Goldscheider, N., Zopfi, J., 2007. Particle-size distribution as indicator for fecal bacteria contamination of drinking water from karst springs. Environmental Science and Technology 41, 8400–8405.

Quiers M., Batiot-Guilhe C., Bicalho CC., Perrette Y., Seidel J.L., S. Van Exter., 2014. Characterisation of rapid infiltration flows and vulnerability in a karst aquifer using a decomposed fluorescence signal of dissolved organic matter. Environmental Earth Sciences, 71, 2, 553-561.

Stedmon, C.A., Seredyńska-Sobecka, B., Boe-Hansen, R., le Tallec, N., Waul, C.K., Arvin, E., 2011. A potential approach for monitoring drinking water quality from groundwater systems using organic matter fluorescence as an early warning for contamination events. Water Research 45, 6030–6038.

Ulloa-Cedamanos, Francesco, Anne Probst, Vanessa Dos-Santos, Thierry Camboulive, Franck Granouillac, and Jean-Luc Probst., 2021. Stream Hydrochemical Response to Flood Events in a Multi-Lithological Karstic Catchment from the Pyrenees Mountains (SW France). Water 13, no. 13: 1818.

5 Hochifen-Gottesacker karst area (test site in Austria)

5.1 General description of the EWS developed

The test site is located in the Northern Alps at the border between Austria (Vorarlberg) and Germany (Bavaria, Fig. 5.1a). The altitude varies between 1035 m asl (Sägebach Spring) and 2230 m asl (summit of Mt. Hochifen). The study site belongs to the Helvetic zone, which plunges on three sides underneath the Flysch nappes consisting of marl and sandstone formations (Wyssling, 1986). The most important rock formation is the Cretaceous Schrattenkalk limestone, which forms the surface of the Gottesacker terrain (Goldscheider, 2005) and constitutes a relatively thin karst aquifer (about 100 m) above a thick marl formation (about 250 m) acting as a regional aquitard (Fig. 5.1b and 5.1c). Previous research (Goldscheider, 2005; Goeppert and Goldscheider, 2008) has shown that the orientation of the underground flow paths is structurally controlled, i.e., the underground flow is parallel to the strata (Fig. 5.1c). The mountain range SE of the Schwarzwasser valley is formed by sedimentary rocks of the Flysch zone and is mainly characterized by low permeability surface drainage. The karst aquifer receives autogenic recharge from precipitation and snowmelt, as well as allogenic recharge from the adjacent Flysch zone sinking into swallow holes near the geologic contact (Chen & Goldscheider, 2014).

Turbulent conduit flow in conduit systems and short residence times lead to a rapid hydraulic and hydrochemical response to rainfall events and therefore to a high vulnerability of the groundwater (Pronk et al., 2007). Due to intense karstification and absence of soil and vegetation in the higher parts of the study site, evapotranspiration is low and a large part of the rainfall contributes to recharge and therefore to spring discharge. Thus, the microbial water quality often varies quickly over a wide range with short-term peaks in bacteria concentrations. Therefore, the need for rapid assessment and near real-time quantification of fecal pollution is apparent (Fiksdal and Tryland, 2008). However, standard cultivation-based methods for the detection and enumeration of fecal bacteria like E. coli require between 18 and 72 hours, depending on the incubation time (Wildeboer et al., 2010), a time frame where many individuals are possibly already exposed to pathogens. The aim is therefore to determine parameters that can be used for an Early-Warning-System (EWS) or at least real-time indicators of fecal contamination at karst springs.

To achieve this, two springs in the Schwarzwasser valley were investigated (Fig. 5.1b and 5.1c). The first one is the large but intermittent Aubach Spring (QA), which discharges up to 8000 L/s but runs completely dry in long dry periods and in winter. Further downstream, the Sägebach Spring (QS, Fig. 5.2) presents the largest permanent spring (base-flow spring) in the valley and discharges up to about 3.5 m^3/s (Chen & Goldscheider, 2014), which is used for a hydropower plant. The total size of the catchment area of QA and QS is about 35 km^2 (Chen & Goldscheider, 2014). Both investigated springs are not used for drinking water supply and show high variability regarding water quality. After rain events, high contamination with fecal bacteria, caused by livestock farming and wildlife, can be observed. Industrial pollution and pesticides do not play a role, since both springs are alpine karst springs and there is no intensive land use in the catchment of the two springs.

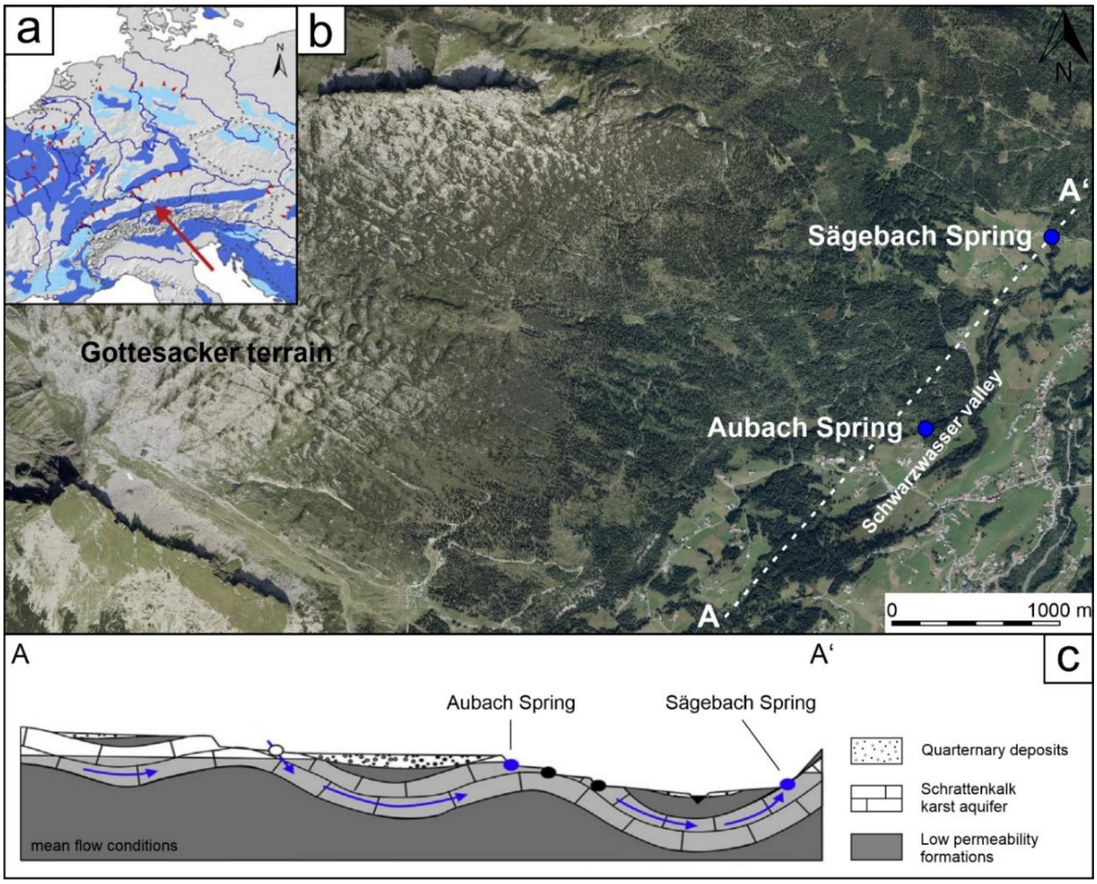

Figure 5.1: a) Location of the test site shown on a section of the World Karst Aquifer Map (Chen et al., 2017) with carbonate rocks in blue b) Detail of the test site with the Gottesacker area and Aubach- and Sägebach Spring (basemap: Land Vorarlberg – data.vorarlberg.gv.at) and c) schematic cross-section with flow paths at mean flow conditions (Goldscheider, 2005) (modified after Goeppert et al., 2020)

Figure 5.2: Sägebach Spring (Photo: Simon Frank)

5.2 Equipment and methods used

At QA and QS, electrical conductivity (EC), water temperature (T), turbidity and total organic carbon (TOC) were continuously monitored during July and August 2020. Additionally, the particle size distribution (PSD) and manual water samples were taken during and immediately after a rainfall event to investigate the influence of hydrological events on the chemical composition and the bacterial content of the spring water.

Detailed information about the used instruments, the data collection procedure and some references related to water quality measurements about the used instruments can be found in Table 5.1.

5.3 Results

At both springs, distinct reactions after rainfall events were recorded for all measured parameters. As an example, the time series for a detailed monitoring period at QS is given in Fig. 5.4 and the statistics for this time period are presented as boxplots in Fig. 5.5.

PSD, turbidity and TOC at QS show a steep increase during the rainfall event (Fig. 5.3), caused by the mobilization of sediments from the karst aquifer by a hydraulic pressure pulse. Indeed, PSD and turbidity show a second peak as well as GLUC activity, while natural fluorescence (Peak A & T), E. coli, ATP and TOC only show one peak. The single peaks of E. coli, natural fluorescence and ATP seem to appear at the same time as the second peak of PSD and turbidity. Hence, the second peak of PSD and turbidity can be attributed to allochthonous sediments.

While the measured EC values during the investigated time period are always below the limit of German Drinking Water Ordinance, the number of bacteria (coliform and E. coli) are permanently above the limit (Fig. 5.4). Also, the TOC values mostly exceed the limit. However, turbidity is partially below the limit but shows a large variation, between 0 and 23.9 NTU, which is indicated by a high number of outliers (Fig. 5.4).

Table 5.1: Detailed information about the used instruments and the data collection procedure at Aubach- and Sägebach Spring. The data collection procedure is represented by the measurement mode, -duration and -interval. NTU = Nephelometric Turbidity Unit, MPN = Most probable number, A.U. = Arbitrary Units, RLU = Relative light units, ***MFU = Modified Fishman Units***

Instrument	Type	Parameter	Unit	Measurement mode	Measurement duration	Measurement interval	Reference with respect to water quality measurements
Field fluorometer	Albillia GGUN-FL30	EC T Turbidity TOC	µS/cm °C NTU mg/L	continuously	2 months	5 min	Schnegg, 2003; Pronk et al., 2007; Goldscheider et al., 2010
Particle counter	Klotz PCSS fluid lite	PSD	µm	continuously	1 month	5 min	Pronk et al., 2007; Ender et al., 2017; Frank et al., 2018
Pressure probe	OTT Orpheus Mini logger	Water level	cm	continuously	2 months	15 min	Frank et al., 2018; Frank et al., submitted
Bacterial content	IDEXX ColiSure Quanti-Tray/2000	*E. coli &* coliforms	MPN/100mL	manually	1 month	~4 hours	Heery et al., 2016; Ender et al., 2017; Frank et al., 2018
TOC analyzer	vario TOC cube	TOC	mg/L	manually	1 month	~4 hours	Frank et al., 2018; Merk et al., 2020
ICP-MS	Agilent Technologies	Cations	mg/L	manually	1 month	~4 hours	Frank et al., 2018; Merk et al., 2020
IC	Dionex system	Anions, except carbonate	mg/L	manually	1 month	~4 hours	Pronk et al., 2007; Goldscheider et al., 2010; Merk et al., 2020
Alkalinity test	Merck test	Carbonate	mg/L	manually	1 month	~4 hours	Frank et al., 2018; Merk et al., 2020
Aqualog	Horiba Aqualog fluorometer	Natural Fluorescence (Peak A & T)	A.U.	manually	1 month	~4 hours	Frank et al., 2018; Sorensen, 2018; Merk et al., 2020
ATP test kit	Hygiena AquaSnap Total test kit	Adenosine triphosphate (ATP)	RLU	manually	4 days	~ 4 hours	Belov et al., 2020; Frank et al., submitted
ColiMinder	ColiMinder Mobile	Enzymatic activity of ß-D-glucuronidase (GLUC activity)	MFU/100mL	continuously	5 days	2 hours	Koschelnik et al., 2015; Frank et al., submitted

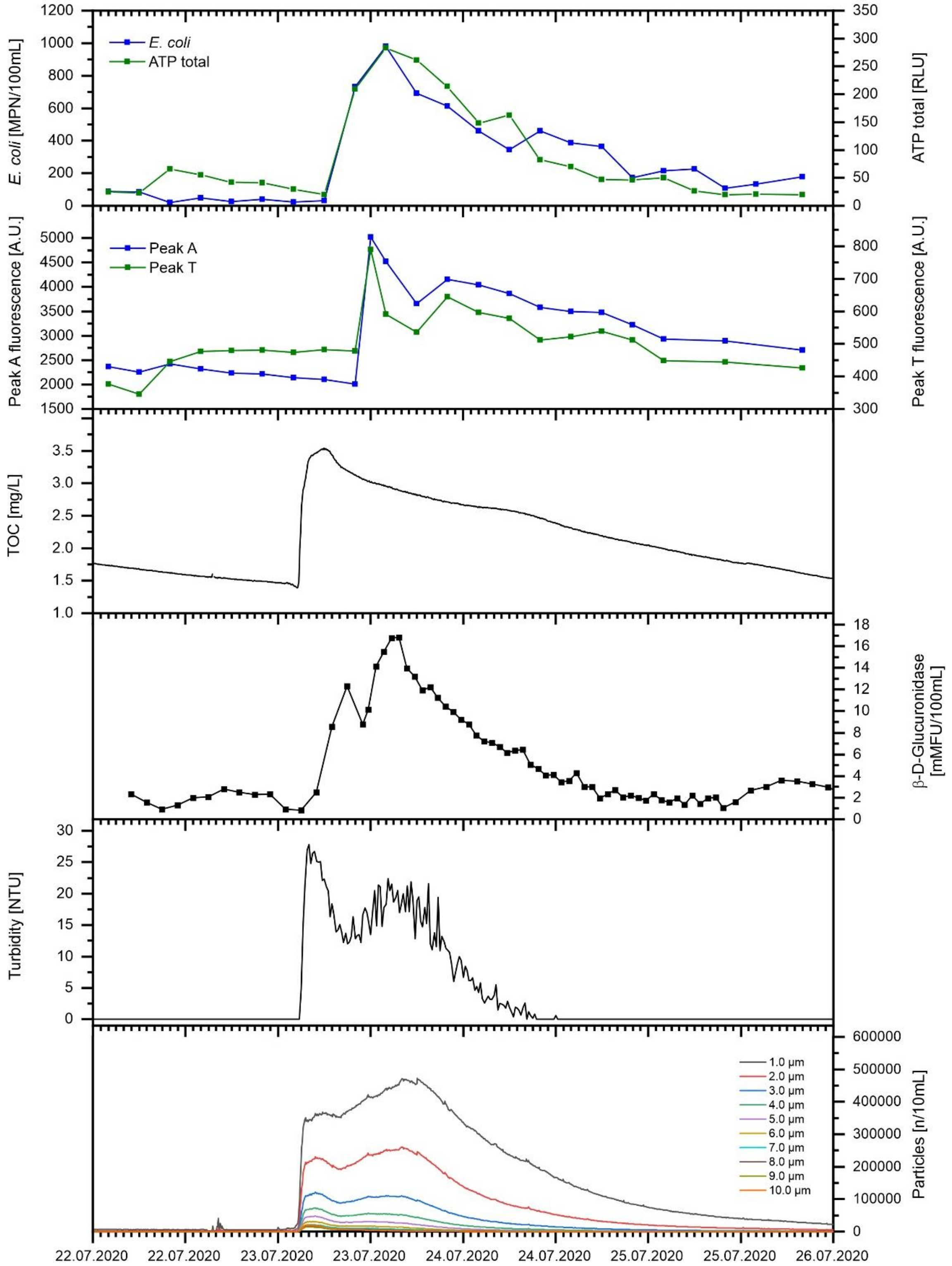

Figure 5.3: Temporal patterns of particle size classes 1 to 10 µm, turbidity, GLUC activity, TOC, E. coli, and fluorescence peaks A and T for Sägebach Spring (Frank et al., submitted)

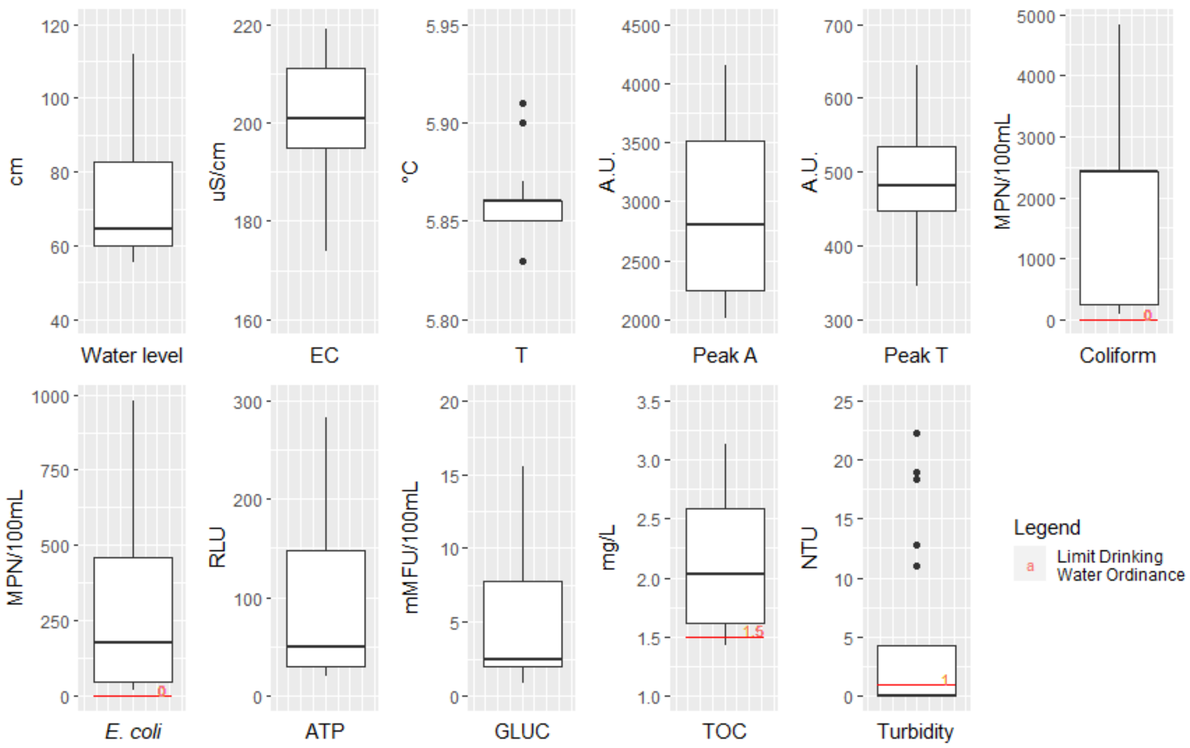

Figure 5.4: Boxplots for water level, electrical conductivity (EC), temperature (T), fluorescence (Peak A & T), bacteria (coliform, E. coli), ATP, GLUC activity, TOC and turbidity for Sägebach Spring. The red lines mark the associated limit of the German Drinking Water Ordinance (data: Frank et al., submitted)

5.4 Discussion

High correlations and simultaneous responses to the rain event of all recorded water quality parameters at QA and QS were found. As an example, the correlations at QS for *E. coli* with all other measured parameters are shown in Table 5.2. The best correlations for *E. coli* were found with small particle-size classes (1-4 µm), Peak T fluorescence and GLUC activity. Therefore, PSD and/or turbidity are suitable parameters for an early-warning system regarding bacterial contamination, because the real *E. coli* contamination occurs during the second peak of these parameters and both can be measured automatically in near real-time. At event scale, GLUC can be used as a real-time indicator of fecal contamination, because GLUC measurements take about 25 minutes but are still significantly faster compared to 24 h for conventional *E. coli* determinations. However, since the GLUC measurements does not deliver the actual *E. coli* quantity, it cannot substitute conventional determination methods.

Table 5.2: Spearman's rank correlation (r_s) with significance (p value) and the number of samples (n) for measured parameters at Sägebach Spring (data: Frank et al., submitted).

Parameter	Correlation with *E. coli* r_s	p value	n
Electrical conductivity	0.9116	< 0.001	21
Peak A	0.9315	< 0.001	21
Peak T	0.6567	< 0.001	21
Coliforms	0.8223	< 0.001	21
ATP	0.6953	< 0.001	21
GLUC	0.747	< 0.001	21
TOC	0.938	< 0.001	21
Turbidity	0.8064	< 0.001	21
1 µm	0.897	< 0.001	21
2 µm	0.9159	< 0.001	21
3 µm	0.925	< 0.001	21
4 µm	0.9315	< 0.001	21
5 µm	0.909	< 0.001	21
6 µm	0.8756	< 0.001	21
7 µm	0.883	< 0.001	21
8 µm	0.8545	< 0.001	21
9 µm	0.8584	< 0.001	21
10 µm	0.8281	< 0.001	21

Legend
0.94
0.90
0.86
0.82
0.78
0.74
0.70
0.64

5.5 Conclusions

Both monitored karst springs in Austria showed a high correlation and a simultaneous response to rain events of all recorded water quality parameters. E. coli concentration correlates best with small particle-size classes, peak T and GLUC. During a rain event at QS, PSD and turbidity show a double peak pattern, while TOC, E. coli and natural fluorescence only show one peak. Due to the high correlation and the double peak pattern, PSD and turbidity, together with GLUC are suitable parameters for an early-warning system regarding bacterial contamination.

The presented results highlight the vulnerability of karst aquifers and demonstrate the need of a high-resolution monitoring in order to record the contamination dynamics. To achieve this, advanced measurement techniques and novel parameters, which are related to fecal contamination and can be measured in near real-time, are needed in order to detect and predict fecal contamination.

5.6 References

Belov A, Vasilyev A, Musenko A (2020) Application of high-voltage discharges for disinfection and activation of irrigation water. Irrig. Drain, 70, 185–19

Chen Z, Goldscheider N (2014) Modeling spatially and temporally varied hydraulic behavior of a folded karst system with dominant conduit drainage at catchment scale, Hochifen–Gottesacker, Alps. Journal of Hydrology. 514: 41-52

Chen Z, Auler A, Bakalowicz M, Drew D, Griger F, Hartmann J, Jiang G, Moosdorf N, Richts A, Stevanovic Z, Veni G, Goldscheider N (2017) The world karst aquifer mapping project: Concept, mapping procedure and map of Europe. Hydrogeol. J. 25 (3), 771-785

Ender A, Goeppert N, Grimmeisen F, Goldscheider N (2017) Evaluation of β-d-glucuronidase and particle-size distribution for microbiological water quality monitoring in Northern Vietnam. Science of The Total Environment 580, 996–1006. https://doi.org/10.1016/j.scitotenv.2016.12.054

Fiksdal I, Tryland I (2008) Application of rapid enzyme assay techniques for monitoring of microbial water quality. Current opinion in Biotechnology 19, 289–294. https://doi.org/10.1016/j.copbio.2008.03.004

Frank S, Fahrmeier N, Goeppert N, Goldscheider N (submitted) High-resolution multi-parameter monitoring of microbial water quality and particles at two alpine karst springs as a basis for an early-warning system

Frank S, Goeppert N, Goldscheider N (2018) Fluorescence-based multi-parameter approach to characterize dynamics of organic carbon, faecal bacteria and particles at alpine karst springs. Science of The Total Environment 615, 1446–1459. https://doi.org/10.1016/j.scitotenv.2017.09.095

Goeppert N, Goldscheider N (2008) Solute and colloid transport in karst conduits under low- and high-flow conditions. Groundwater 46 (1), 61-68

Goeppert N, Goldscheider N, Berkowitz B (2020) Experimental and modeling evidence of kilometer-scale anomalous tracer transport in an alpine karst aquifer. Water research, 178.

Goldscheider, N (2005) Fold structure and underground drainage pattern in the alpine karst system Hochifen-Gottesacker. Eclogae geol. Helv. 98 (1), 1–17

Goldscheider N, Pronk M, Zopfi J (2010) New insights into the transport of sediments and microorganisms in karst groundwater by continuous monitoring of particle-size distribution. Geol Cro 63, 137–142. https://doi.org/10.4154/gc.2010.10

Heery B, Briciu-Burghina C, Zhang D, Duffy G, Brabazon D, O'Connor N, Regan F (2016) ColiSense, today's sample today: A rapid on-site detection of β-d-Glucuronidase activity in surface water as a surrogate for E. coli. Talanta 148, 75–83. https://doi.org/10.1016/j.talanta.2015.10.035

Koschelnik J, Vogl W, Epp M, Lackner M (2015) Rapid analysis of β-D-glucuronidase activity in water using fully automated technology. Presented at the water resources management 2015, A Coruña, Spain, pp. 471–481. https://doi.org/10.2495/WRM150401

Merk M, Goeppert N, Goldscheider N (2020) Processes Controlling Spatial and Temporal Dynamics of Spring Water Chemistry in the Black Forest National Park, Science of The Total Environment 723, 137742, https://doi.org/10.1016/j.scitotenv.2020.137742

Pronk M, Goldscheider N, Zopfi J (2007) Particle-size distribution as indicator for fecal bacteria contamination of drinking water from karst springs. Environmental science & technology, 41(24), 8400-8405

Schnegg, P.-A. (2003) A new field fluorometer for multi-tracer tests and turbidity measurement applied to hydrogeological problems. In

Proceedings of the eight International Congress of the Brazilian. Geophysical Society. https://doi.org/10.3997/2214-4609-pdb.168.arq_167

Sorensen J.P.R. (2018) Online fluorescence spectroscopy for the real-time evaluation of the microbial quality of drinking water. Water Research 9

Wildeboer d, amirat l, Price R.G, Abuknesha R.A (2010) Rapid detection of Escherichia coli in water using a hand-held fluorescence detector. Water research 44, 2621–2628. https://doi.org/10.1016/j.watres.2010.01.020

Wyssling G (1986) Der frühkretazische Schelf in Vorarlberg und im Allgäu - Stratigraphie, Sedimentologie und Paläogeographie. Jb. Geol. B.-Anst. 129, 161-265

6 Conclusions

Four different study cases were investigated in the framework of KARMA project in order to identify groundwater quality issues and to acquire new knowledge about the development of Early Warning Systems. KARMA partners used different approaches for this study: in the study cases of Italy and Austria, temporal monitoring stations were set at event scale. On the other hand, continuous records of (at least) 17 parameters in France exist given that monitoring station has been maintained since 2015. In Spain study case it began at the end of 2020.

Fluorescence methods have proven to be an ideal tool for the detection of contaminants given its measurement rapidness and versatility for its application in different environments. The application of this methodology has been a common feature in all four KARMA EWS study cases. However, other complementary techniques have been used depending on the project partner. Those complementary techniques include the continuous record of physico-chemical parameters, Radon-222, NO_3^-, Particle Size Distribution (PSD) or laboratory analysis for the determination of major ions, Total Organic Carbon (TOC), trace metals and total coliforms or E. coli.

A common stage has then been achieved at the four test sites: the identification of (1) potential hazardous substances for human health and (2) “Early Warning” parameters, those that show a good correlation with contamination indicators. Although each study case presents different geological particularities and contaminant sources, all of them show a problem regarding suspended sediment transport. Maximum turbidity records vary from ≈140 NTU at Vitella D'Oro spring (Italy), ≈60 NTU at Cornicabra spring, ≈300 NTU at Algarrobal spring (Spain), ≈150 NTU at Lez spring (France) and ≈25 at Sägebach spring (Austria).

However, a more advanced stage of EWS development has been achieved at two test sites with the definition of the main EWS workflow and specific thresholds that activate the alerts. In addition, the validation of selected thresholds in order to test the robustness of the respective systems for reliably predicting the occurrence of contamination events has been started and supposes a continuous process. Furthermore, EWS validation tools also include the verification of protection zones and contaminant travel times in karst areas through specific techniques such as tracer experiments.

Given that the development of this type of prevention systems in karst aquifers is still limited and that water stress in the Mediterranean region is expected to increase, the experience acquired in KARMA project serves as basis for future researches.